

1 **Silver contents and Cu/Ag ratios in Martian meteorites and the**
2 **implications for planetary differentiation**

3

4 Zaicong Wang^{#*} and Harry Becker

5

6 Freie Universität Berlin, Institut für Geologische Wissenschaften, Malteserstrasse 74-100, 12249,

7 Berlin, Germany

8 [#]Present address: State Key Laboratory of Geological Processes and Mineral Resources, School of

9 Earth Sciences, China University of Geosciences, 388 Lumo Road, Hongshan District, 430074, Wuhan,

10 China

11 ^{*}Correspondence to: Zaicong Wang (email: wzc231@163.com)

12

13 **Abstract:**

14 Silver and Cu show very similar partitioning behavior in sulfide melt-silicate melt
15 and metal-silicate systems at low and high pressure-temperature (P-T) experimental
16 conditions, implying that mantle melting, fractional crystallization and core-mantle
17 differentiation have at most modest (within a factor of 3) effects on Cu/Ag ratios. For this
18 reason, it is likely that Cu/Ag ratios in mantle-derived magmatic products of planetary bodies
19 reflect that of the mantle and, in some circumstances, also the bulk planet composition. To
20 test this hypothesis, new Ag mass fractions and Cu/Ag ratios in different groups of Martian
21 meteorites are presented and compared with data from chondrites and samples from the
22 Earth's mantle.

23 Silver contents in lherzolithic, olivine-phyric and basaltic shergottites and nakhlites
24 range between 1.9 and 12.3 ng/g. The data display a negative trend with MgO content and
25 correlate positively with Cu contents. In spite of displaying variable initial $\epsilon^{143}\text{Nd}$ values and
26 representing a diverse spectrum of magmatic evolution and physiochemical conditions,
27 shergottites and nakhlites display limited variations of Cu/Ag ratios (1080 ± 320 , 1s, $n=14$).
28 The relatively constant Cu/Ag suggests limited fractionation of Ag from Cu during the
29 formation and evolution of the parent magmas, irrespectively of whether sulfide saturation
30 was attained or not. The mean Cu/Ag ratio of Martian meteorites thus reflects that of the
31 Martian mantle and constrains its Ag content to 1.9 ± 0.7 ng/g (1s).

32 Carbonaceous and enstatite chondrites display a limited range of Cu/Ag ratios of
33 mostly 500-2400. Ordinary chondrites show a larger scatter of Cu/Ag up to 4500, which may
34 have been caused by Ag redistribution during parent body metamorphism. The majority of
35 chondrites have Cu/Ag ratios indistinguishable from the Martian mantle value, indicating that
36 Martian core formation strongly depleted Cu and Ag contents, but probably did not
37 significantly change the Cu/Ag ratio of the mantle compared to bulk Mars. Bulk Mars is
38 richer in moderately volatile elements than Earth, however, the Martian mantle displays a
39 much stronger depletion of the moderately volatile elements Cu and Ag, e.g., by a factor of 15
40 for Cu. This observation is consistent with experimental studies suggesting that core
41 formation at low P-T conditions on Mars led to more siderophile behavior of Cu and Ag than
42 at high P-T conditions as proposed for Earth. In contrast, Cu/Ag ratios of the mantles of Mars
43 and Earth ($\text{Cu/Ag}_{\text{Earth}}=3500 \pm 1000$) display only a difference by a factor of 3, which implies
44 restricted fractionation of Cu and Ag even at high P-T conditions. The concentration data

45 support the notion that siderophile element partitioning during planetary core formation scales
46 with the size of the planetary body, which is particularly important for the differentiation of
47 large terrestrial planets such as Earth. Collectively, the Ag and Cu data on magmatic products
48 from the mantles of Mars and Earth and the data on chondrites confirm experimental
49 predictions and support the limited fractionation of Cu and Ag during planetary core
50 formation and high-temperature magmatic evolution, and probably also in early solar nebular
51 processes.

52

53 **Keywords:** Mars, shergottites, Cu/Ag ratio, core formation, planetary differentiation

54

1. Introduction

During planetary core formation, siderophile elements were distributed between the cores and mantles of differentiated planetesimals and planets according to their metal-silicate and sulfide-silicate partition coefficients (e.g., Jones and Drake, 1986; O'Neill, 1991). Experimental studies of siderophile element partitioning between metal, sulfide and silicate melt at low- and high-pressure (P) - temperature (T) conditions now permit to constrain the P-T- f_{O_2} conditions of planetary accretion and core formation of different planetary bodies, such as Earth, Moon and Mars (e.g., Corgne et al., 2008; Fischer et al., 2015; Laurenz et al., 2016; Li and Agee, 1996; Li and Agee, 2001; Mann et al., 2009; Righter, 2011; Rubie et al., 2011; Rubie et al., 2015; Rubie et al., 2016; Siebert et al., 2011; Wade and Wood, 2005; Wood, 2008). Accurate estimates of the contents of siderophile elements in the mantle and in the core are essential for a successful application of this approach.

The contents of siderophile elements in the mantle can be constrained directly by rock samples from planetary mantles if such samples are available, for instance, mantle peridotites in the case of the Earth. However, planetary cores are inaccessible and thus the contents of siderophile elements in planetary cores are often calculated by subtraction of mantle element inventories from assumed chondritic model compositions of the bulk planet (McDonough, 2014). This approach appears to be valid for refractory elements with uncertainties of approximately a few percent (such as rare earth elements and refractory siderophile elements, e.g., Dauphas and Pourmand, 2015; Palme and O'Neill, 2014). For volatile elements (the elements with the 50% condensation temperature at 10^{-4} bar total pressure less than those of

76 Mg, Si and Fe, Lodders, 2003), uncertainties in the exact composition of the building
77 materials of the planets may be much larger, because chondritic materials display much larger
78 variations in volatile element abundances (e.g., Wasson and Kallemeyn, 1988) and the
79 behavior of these elements in chondrites is decoupled from refractory elements (e.g., Davis,
80 2006; Kadlag and Becker, 2015). Furthermore, it cannot be excluded that the fractionation of
81 volatile elements in the building materials of the terrestrial planets was different from that in
82 chondrites (e.g., Dauphas, 2017; Wang et al., 2016) and that additional volatile loss processes
83 may have occurred during planetary accretion (e.g., Canup et al., 2015; Wang and Jacobsen,
84 2016). The high contents of volatile S and K on Mercury (Nittler et al., 2011; Peplowski et al.,
85 2011) are also not easily reconciled with models that predict that the volatile depletion of
86 planetary bodies increases as heliocentric distances decrease (McCubbin et al., 2012).

87 Experimentally determined high P-T metal-silicate partitioning data (e.g., 5-20 GPa
88 and 2000-2300 °C) can be applied directly to Mars-size planetary bodies (e.g., Corgne et al.,
89 2008; Fischer et al., 2015; Laurenz et al., 2016; Li and Agee, 2001; Mann et al., 2009; Righter,
90 2011; Rubie et al., 2011; Siebert et al., 2011; Wade and Wood, 2005). In forward models,
91 such experimental results and data on the concentration of siderophile volatile elements
92 (volatile elements with metal affinity during metal-silicate partitioning) in planetary mantles
93 may provide independent constraints on the likely composition of accreted materials (e.g.,
94 Wang et al., 2016). The core formation history of planetary bodies likely involves changes in
95 P-T- fO_2 conditions (e.g., Wade and Wood, 2005; Rubie et al., 2011; 2015). Thus, it is best to
96 first consider the siderophile volatile elements whose siderophile element ratios are little

97 affected by core formation. In such cases, the ratios of siderophile elements in the mantle
98 should reflect the ratios in the bulk planetary body.

99 Experimental data on metal-sulfide-silicate partitioning suggest that Ag and Cu very
100 likely display such behavior (Vogel, 2015; Wood et al., 2014). Sulfide melt-silicate melt
101 partitioning data have also indicated no systematic fractionation of Cu from Ag in sulfide
102 melt-silicate melt systems, in spite of the large variations of partition coefficients at different
103 physicochemical conditions (Kiseeva and Wood, 2013; Kiseeva and Wood, 2015; Li and
104 Audetat, 2012). Therefore, magmatic products originating from the mantle likely retain the
105 Cu/Ag ratio of their mantle source and also the value of the bulk planetary body. In order to
106 test this hypothesis, we present Ag concentration data on Martian meteorites and new Ag and
107 Cu data on some ordinary chondrites obtained by isotope dilution ICP-MS. The data on
108 Martian meteorites are compared with terrestrial samples and chondrites and the behavior of
109 Cu and Ag in these objects is discussed.

110 **2. Samples and methods**

111 About 0.2-0.25 gram fragments of 15 Martian meteorites were obtained (Table 1).
112 Except for Sau 005, these samples are falls and finds from the cold desert of Antarctica, with
113 negligible terrestrial alteration (Wang and Becker, 2017). The meteorites consist of diverse
114 groups of lherzolitic (n=2), olivine-phyric (n=8) and basaltic (n=1) shergottites, nakhlites
115 (n=3) and the orthopyroxenite cumulate ALH 84001, with a large range of presumed
116 formation ages from 4.1 Ga to 150 Ma (Lapen et al., 2010; Nyquist et al., 2001). Based on
117 lithophile incompatible elements and radiogenic isotopes of Sr, Nd and Os, they reflect a

118 range of geochemical characteristics with substantial differences in mantle source
119 compositions of lithophile incompatible elements, variations in the degrees of Martian crustal
120 contamination and magmatic evolution at variable oxygen fugacity (e.g., Brandon et al., 2012;
121 Herd et al., 2002; Lapen et al., 2010; Meyer, 2013; Mittlefehldt, 1994; Treiman, 2005;
122 Wadhwa, 2008).

123 These samples have been used to measure Cu, S, Se and Te contents by isotope
124 dilution ICP-MS after digestion in Parr digestion bombs (Wang and Becker, 2017). In the
125 present study, the Ag contents were determined by isotope dilution ICP-MS from the same
126 digested sample aliquots (Tables 1 and 2). Obtaining both Cu and Ag contents from the same
127 sample aliquots reduces the effect of separation of small-scale monosulfide solid solution
128 (MSS)-sulfide liquid (if they occur at all) and the effect of the heterogeneous distribution of
129 trace sulfides, which cause scatter in abundances and ratios of chalcophile elements if the
130 latter are analyzed in different aliquots of bulk rocks.

131 The Ag and Cu abundances in nine ordinary chondrites were also determined from
132 the same sample aliquots in order to compare with literature Ag and Cu data on ordinary
133 chondrites which display a large range of Cu/Ag. The analyzed chondrites are mostly
134 meteorite falls, with negligible terrestrial contamination, and include the H, L and LL groups
135 with different degrees of parent body metamorphism (Table 3,
136 <https://www.lpi.usra.edu/meteor/metbull.php>). Because the literature data show a larger range
137 of Cu/Ag ratios in ordinary chondrites than in carbonaceous and enstatite chondrites and
138 alteration potentially affects Ag contents (and thus Cu/Ag, see below), the new data from

139 ordinary chondrites falls may constrain whether the scatter of Cu/Ag of ordinary chondrites
140 from the literature reflects a pristine feature or is due to terrestrial alteration.

141 Sample preparation and digestion have been described before (Wang and Becker,
142 2017; Wang et al., 2015) and only a brief outline of the method is given here. Fragments of
143 Martian meteorites were crushed to smaller fractions using an agate mortar and then
144 processed to fine powder in a Retsch® oscillating ball mill MM 200 with agate cups.
145 Ordinary chondrites were crushed to powder in an agate mortar. After addition of spike
146 solutions containing ^{109}Ag - ^{65}Cu and spikes of other elements such as S, Se and Te, sample
147 powders were digested in a mixture of concentrated HF-HNO₃ in Parr digestion bombs at
148 190°C for 3 days. The digestion solution was dried down and converted to chloride form. The
149 sample solution was dissolved in 4.5 mol l⁻¹ HCl and then loaded on 2 ml 100-200 mesh
150 pre-cleaned Eichrom 1-X8 anion resin to remove matrix elements and elements that may form
151 interferences (Wang et al., 2015).

152 Martian meteorites have low Ag contents (Tables 1 and 2) and very high Zr/Ag and
153 Nb/Ag ratios, particularly in incompatible element-enriched samples (e.g., Meyer, 2013;
154 Yang et al., 2015). In order to reduce the effect of the oxide interferences on Ag isotopes, 9
155 mol l⁻¹ HCl was used to exclusively collect Ag after elution of matrix in 4.5 mol l⁻¹ HCl, 0.4
156 mol l⁻¹ HCl and 0.05 mol l⁻¹ HCl. Because of low Zr/Ag and Nb/Ag in chondrites, the Ag
157 fraction of ordinary chondrites was collected with other elements of interest (Cd and Tl) in a
158 mixture of 0.7 mol l⁻¹ HNO₃ and 1 vol.% H₂O₂ (Wang et al., 2015). After conversion to nitric
159 acid form, the samples were dissolved in 0.28 mol l⁻¹ HNO₃ and analyzed at Freie Universität
160 Berlin on the Element XR sector field ICP-MS (Thermo Scientific) coupled to an Aridus-I

161 desolvator to limit oxide formation ($\text{CeO}^+/\text{Ce}^+ < 0.002$). At such conditions, a 20 ng/g Nb
162 standard solution yielded $^{93}\text{NbO}^+/\text{Nb}^+$ of < 0.0002 . The monitored $^{91}\text{Zr}/^{107}\text{Ag}$ and $^{93}\text{Nb}/^{109}\text{Ag}$
163 in Martian meteorites were low and mostly < 0.1 , indicating negligible effects of these
164 metal-oxide interferences. Different reference materials (e.g., NIST SRM 612 glass, BHVO-1,
165 BHVO-2 and others) and the replicates have yielded reproducible results ($< 5\%$, 2s, Wang et
166 al., 2015). During the period of sample measurements, the total procedural blanks (also by
167 isotope dilution, $n=5$, 2s) were 0.022 ± 0.015 ng Ag and 4 ± 4 ng Cu. Procedural blank
168 corrections were applied, and blank contributions range from mostly $< 3\%$ to 8% for the
169 largest correction for Ag and 28% for Cu (Table 1).

170

3. Results

171 *3.1.1. Martian meteorites*

172 The new data on Martian meteorites are listed in Table 1 and plotted in Figure 1.
173 Overall, the Ag contents in shergottites increase from Iherzolitic, olivine-phyric to basaltic
174 types, with a range of 1.9 ng/g to 12.3 ng/g (Figure 1). Three nakhlite samples have 7.8 ng/g
175 to 10.5 ng/g Ag. ALH84001 has an Ag content of 7.2 ng/g.

176 Silver data in the Martian meteorites have been reported before (Biswas et al., 1980;
177 Kong et al., 1999; Laul et al., 1972; Laul et al., 1986; Lodders, 1998; Meyer, 2013; Smith et
178 al., 1984; Treiman et al., 1986; Wang et al., 1998; Yang et al., 2015). Our new Ag data are
179 within the range of literature data but tend to be lower, even in the same samples. For
180 example, Zagami has 8.1 ng/g in this work, compared to 14.2 ng/g (Treiman et al., 1986), 31
181 ng/g (Wang et al., 1998) or 12.4 ng/g (Kong et al., 1999) in previous work (Table 2). A

182 similar behavior was observed for Nakhla, with 32 ng/g (Wang et al., 1998), 40 ng/g (Laul et
183 al., 1972) or 246 ng/g (Kong et al., 1999) in previous work compared to 7.8 ng/g in the
184 present study. The different aliquots of ALHA 77005 have similar values at 4-5 ng/g (Table
185 2), whereas our Ag concentration of 7.2 ng/g in ALH 84001 is much higher than the previous
186 values of 0.22-0.35 ng/g (Wang et al., 1998) and < 0.9 ng/g (Kong et al., 1999).

187 The observation that different studies obtained different Ag concentrations in
188 different aliquots of the same samples has also been noted for other chalcophile elements, e.g.,
189 S (e.g., Ding et al., 2015; Franz et al., 2014; Wang and Becker, 2017), Cu (Meyer, 2013;
190 Wang and Becker, 2017) and the highly siderophile elements (HSE, e.g., Brandon et al., 2012;
191 Jones et al., 2003; Yang et al., 2015). The scatter of data may reflect uncertainties of the
192 applied analytical methods and sample heterogeneity as different proportions of silicate
193 phenocrysts and sulfides may be present in different aliquots of the same sample. Some Ag
194 concentration data on bulk rocks of shergottites from the literature were produced by laser
195 ablation ICP-MS with a relatively high detection limit of 2 ng/g for Ag (Yang et al., 2015).
196 Most samples analyzed by the latter method show high Ag contents (up to 651 ng/g). For
197 example, Zagami has 651 ng/g Ag (Yang et al., 2015), far higher than our value and data
198 obtained by others (Table 2). A possible explanation for such very high concentrations might
199 be interferences from transition metal oxides, e.g., ⁹¹ZrO and ⁹³NbO.

200 Similar to Cu abundances, Ag contents display a broad negative trend with MgO
201 contents (Figure 1), and, not surprisingly, Ag and Cu are positively correlated. Because Ag
202 and Cu contents of the present study are from the same sample aliquots, the effect of sample
203 heterogeneity on Cu/Ag ratios is limited. If ALH 84001 is not considered, the Martian

204 meteorites display limited variation in Cu/Ag ratios with a mean value of 1080 ± 320 (1s, n=14,
205 Figure 2). Of these samples, Y-980459 and LAR 06319 are thought to be closed-system
206 crystallization products of primitive magma from the Martian mantle (Basu Sarbadhikari et al.,
207 2009; Mikouchi et al., 2004; Musselwhite et al., 2006; Usui et al., 2012). The Cu/Ag ratios of
208 Y-980459 (1122 ± 31) and LAR 06319 (1474 ± 48) are similar to the mean value within
209 uncertainty. Sau 005 (628 ± 14) and Y-00593 (466 ± 9) tend to have the lowest Cu/Ag ratios and
210 some olivine-phyric shergottites have slightly higher values of around 1500. Olivine-phyric
211 shergottites which were derived from mantle reservoirs with different depletion of
212 incompatible lithophile elements show no obvious difference in Cu/Ag ratios (range from
213 1100 to 1500, Table 1, Figure 3).

214 **3.1.2. Chondrites**

215 Here we present new data on some ordinary chondrites and also compiled literature
216 data of Cu and Ag contents in chondrites. Mean contents of Cu and Ag in different groups of
217 chondrites display no systematic variations or differences (Wasson and Kallemeyn, 1988).
218 Mean Cu/Ag ratios in carbonaceous (CI, CM, CV and CO), ordinary (H, L and LL) and EH
219 chondrites are also similar, however, EL chondrites show higher Cu/Ag (Wasson and
220 Kallemeyn, 1988, Figure 4). Literature data where both Cu and Ag contents were obtained
221 from the same samples, indicate that Cu/Ag ratios of CI, CM, CO, CV, EH and EL chondrites
222 range from 500 to 2400 (a mean of 1100 ± 400 , 1s, n=24, Figure 4). The mean Cu/Ag of EL
223 chondrites in which Cu and Ag were determined on different samples (4780, Wasson and
224 Kallemeyn, 1988) is different from Cu/Ag values of EL chondrites for which Cu and Ag
225 concentration data were obtained from the same sample (a mean Cu/Ag of 1260 ± 670 , 1s,

226 n=5). This suggests that it is important to obtain Cu and Ag data on the same samples, or
227 better, from the same sample aliquot.

228 Ordinary chondrites show a large scatter of Cu/Ag ratios from 200 to 4500 (mean =
229 1600 ± 1000 , 1s, n=39, median = 1400), however, the majority of samples have Cu/Ag
230 similar to carbonaceous and enstatite chondrites (Figure 4). The scattered Cu/Ag is mainly
231 due to the large variation in Ag contents (e.g., Friedrich et al., 2004; Kaczaral et al., 1989;
232 Koblitz, 2005; Lingner et al., 1987; Schönbächler et al., 2008; Schaefer and Fegley, 2010;
233 Wolf and Lipschutz, 1995; Wolf et al., 1997). The new Cu and Ag contents in ordinary
234 chondrites are listed in Table 3 and are shown in Figure 4. The samples are mostly falls and
235 vary from petrological type 3 to 6 (<https://www.lpi.usra.edu/meteor/metbull.php>). Our results
236 show a range of Cu/Ag ratios similar to the literature data on ordinary chondrites. Samples of
237 this study do not show systematic differences or changes of Cu/Ag with the petrological type
238 or as a function of ordinary chondrite group.

239 **4. Discussion**

240 **4.1. The effect of Martian crustal contamination and terrestrial alteration**

241 Based on $\Delta^{33}\text{S}$ (Franz et al., 2014) and δD values (Usui et al., 2012), some Martian
242 meteorites or their parent magmas underwent variable extents of contamination by Martian
243 crustal materials. These contamination processes barely affected Cu, Se, Te and HSE contents
244 but might have increased S contents because of incorporation of sulfate on Mars (Farquhar et
245 al., 2000; Franz et al., 2014; Greenwood et al., 2000; Wang and Becker, 2017). Terrestrial
246 alteration may increase Ag contents as indicated by Ag concentration data on serpentinized

247 peridotites and komatiites (Theis et al., 2013; Wang and Becker, 2015), probably because of
248 the mobile behavior of Ag during hydrothermal or other fluid-controlled processes (Wang and
249 Becker, 2015). Therefore, the effect of Martian crustal contamination and terrestrial alteration
250 should be evaluated for Ag contents and Cu/Ag ratios in Martian meteorites.

251 The literature values of Ag contents in ALH 84001 are 0.22 and 0.35 ng/g (Wang et
252 al., 1998), consistent with the very low contents of the other strongly chalcophile elements
253 HSE, Cu, Se and Te (Jones et al., 2003; Wang and Becker, 2017). The low contents of HSE,
254 Cu and Se in the cumulate ALH 84001 imply a very low sulfide abundance and low Ag and S
255 contents. However, the present study shows a higher Ag content of 7.2 ng/g in ALH 84001.
256 The high Ag content is coupled with a high S content of 219 $\mu\text{g/g}$ in the same sample aliquot
257 (Wang and Becker, 2017), possibly indicating an effect of Martian crustal assimilation on Ag
258 as it was suggested for S. Some other SNC samples such as MIL 03346, RBT 04262 and LAR
259 06319 also display evidence from $\Delta^{33}\text{S}$ (Franz et al., 2014) and high S/Se (Wang and Becker,
260 2017) that their S budget was affected significantly by contamination with Martian crust.
261 Although the contamination affects the S budget, these samples show Cu/Ag similar to the
262 others with little or no contamination with sulfur from the Martian crust. Therefore, the effect
263 of Martian crustal contamination is likely to be also limited for Ag as for the HSE, Cu, Se and
264 Te. The specific reason for the relatively high Ag content of ALH 84001 in this study is
265 unclear.

266 Sau 005 (628 ± 14) and Y-000593 (466 ± 9) are both meteorite finds and have the
267 lowest Cu/Ag ratios in samples of this study, a factor of 2 lower than the mean value. The
268 lower Cu/Ag in both samples may be explained by terrestrial alteration, however, Ag contents

269 of these two samples display no obvious difference from other samples and are relatively low
270 (around 9-12 ng/g) and other chalcophile element ratios did not yield clear evidence for a
271 significant influence of terrestrial weathering on these elements (Wang and Becker, 2017).
272 Alternatively, the range of variations of Cu/Ag recorded by the SNC meteorites reflects
273 intrinsic variations in the parent magmas and in the Martian mantle.

274 **4.2. Limited fractionation of Ag and Cu in magmatic processes**

275 During high-temperature magmatic processes, Ag and Cu are mainly controlled by
276 sulfide melt-silicate melt partitioning (e.g., Kiseeva and Wood, 2015; Li and Audetat, 2012;
277 Wang and Becker, 2015). Experimental results have indicated no significant or systematic
278 fractionation of Cu from Ag in sulfide melt-silicate melt systems, regardless of the
279 physicochemical conditions (Figure 5, Kiseeva and Wood, 2013; Kiseeva and Wood, 2015; Li
280 and Audetat, 2012). The only exception where large differences between Cu and Ag
281 partitioning may occur is the segregation of MSS from sulfide melt (e.g., Bockrath et al.,
282 2004; Li and Audetat, 2012), a process which is restricted to specific situations during the late
283 cooling stage of some basic magma series (e.g., Dare et al., 2011; Patten et al., 2013), some
284 supra-subduction zone magmatic systems (e.g., Jenner et al., 2010) and the exsolution of
285 sulfide melts into different sulfide phases during cooling of mantle rocks (e.g., Alard et al.,
286 2000; Luguet et al., 2004).

287 Many Martian meteorites of this study are magmatic cumulates with variable
288 proportions of interstitial basic melts. Based on rare earth element patterns and Sr-Nd-Os
289 isotopes, they originated from different mantle sources and show a large range of
290 emplacement ages and variable magmatic evolution (e.g., Brandon et al., 2012; Herd et al.,

291 2002; Lapen et al., 2010; Meyer, 2013; Mittlefehldt, 1994; Treiman, 2005; Wadhwa, 2008).
292 Nevertheless, they display a restricted range of Cu/Ag ratios (466 to 1527 with a mean of
293 1080 ± 320 , Table 1 and Figures 2-3), similar to ratios of some other chalcophile elements (e.g.,
294 Cu/Se, Wang and Becker, 2017). These features suggest limited fractionation of Ag from Cu
295 at different magmatic conditions on Mars.

296 Recent work suggested a sulfide-undersaturated evolution of the parent magmas of many
297 Martian meteorites (Ding et al., 2015; Wang and Becker, 2017). The increasing Ag and Cu
298 contents with decreasing MgO support a sulfide undersaturated evolution of Martian magmas
299 (Figure 1; Wang and Becker, 2007). Given such conditions, it is not surprising that different,
300 even genetically unrelated Martian meteorites show similar Cu/Ag. Because Cu and Ag are
301 incompatible elements during melting of mantle in which sulfides are not retained and during
302 the subsequent evolution of sulfide-undersaturated mantle-derived magmas (Cu and Ag are
303 incompatible in olivine and pyroxenes, e.g., Fellows and Canil 2012; Lee et al., 2012; Liu et
304 al., 2014), these elements become depleted or enriched in constant proportion in cumulates,
305 evolving silicate melts and mixtures of cumulates and melts (as in most SNC meteorites).
306 Therefore, no significant change of Cu/Ag ratios should have occurred in lherzolitic,
307 olivine-phyric, basaltic shergottites, and at least some nakhlites, even though concentrations
308 of Cu and Ag may vary (Figures 1 and 2). At sulfide-saturated conditions, Cu and Ag also
309 would display little fractionation because Ag and Cu have similar sulfide melt-silicate melt
310 partition coefficients for a large range of FeO contents in silicate magmas (Figure 5). During
311 slow cooling of silicate magma and the formation of immiscible sulfide droplets, Cu and Ag
312 may fractionate differently if MSS forms at low temperatures and separates from sulfide melt

313 (e.g., Dare et al., 2011; Patten et al., 2013). In the MSS-sulfide melt system, Ag tends to
314 enrich in the remaining sulfide liquid more strongly than Cu (Jenner et al., 2010; Li and
315 Audetat, 2012). Because sulfides in shergottites and nakhlites mainly crystallized during the
316 late stage of cooling and crustal emplacement and a limited amount of chalcopyrites exsolved
317 during cooling (e.g., Chevrier et al., 2011; Lorand et al., 2005), the petrological observations
318 and the limited Cu/Ag range of the present study indicate that MSS-sulfide melt segregation
319 likely did not play a significant role in the fractionation of Cu/Ag and other chalcophile
320 elements in bulk rocks of Martian meteorites.

321 Although factors such as FeO content in the silicate melt and sulfide composition
322 strongly affect partition coefficients, this is not the case for Cu and Ag during sulfide
323 melt-silicate melt partitioning (Kiseeva and Wood, 2013; Kiseeva and Wood, 2015; Li and
324 Audetat, 2012, Figure 5d). The mean Cu/Ag ratios in fresh terrestrial lherzolites, MORB from
325 different ocean basins and sulfide droplets in MORB are similar (Figure 2). Although
326 MORBs undergo substantial sulfide melt-silicate melt fractionation and display variable Cu
327 contents, existing data indicate limited changes in Cu/Ag during partial melting,
328 melt-peridotite reaction and fractional crystallization processes in the Earth's convecting
329 mantle and predominant control of Cu/Ag and other chalcophile element ratios by sulfide
330 melt-silicate melt partitioning (e.g., Jenner and O'Neill, 2012; Jenner et al., 2010; Patten et al.,
331 2013; Wang and Becker, 2015). We note that in some terrestrial peridotites (notably those
332 with low Cu and Ag abundances), Cu/Ag ratios are substantially lower (Figure 2), which may
333 reflect preferential enrichment of Ag during serpentinization and other forms of alteration

334 (Wang and Becker, 2015). This is the main reason why some peridotites show low Cu/Ag
335 ratios relative to those with similar MgO contents (Figure 2).

336 The mantles of Earth and Mars are characterized by different oxygen fugacity
337 conditions, FeO, Ni and Cu contents. In particular, because of the higher FeO contents of
338 Martian magmas (e.g., 18 wt.%) relative to terrestrial magmas (e.g., 10 wt.%), sulfur contents
339 at sulfide saturation of mantle-derived magmas on Mars are much higher than those on Earth
340 at similar P-T conditions (e.g., 3500-4000 $\mu\text{g/g}$ S versus 1500-2000 $\mu\text{g/g}$, Ding et al., 2015;
341 Liu et al., 2007; Righter et al., 2009; Smythe, et al., 2017; references therein). This leads to a
342 different role of sulfide melt-silicate melt partitioning in these planets. On Mars, because of
343 high sulfur contents at sulfide saturation, most mantle-derived magmas were
344 sulfide-undersaturated from the source to subsequent high-temperature crystallization stage in
345 the crust (Ding et al. 2015, Wang and Becker, 2017). In contrast, most terrestrial basic
346 magmas should be sulfide-saturated during partial melting and during subsequent fractional
347 crystallization (e.g., Czamanske and Moore, 1977; Fortin et al., 2015; Liu, et al., 2007;
348 Lorand, 1989; Patten et al., 2013; Smythe et al., 2017). The limited range in Cu/Ag of
349 Martian meteorites and the coincidence in Cu/Ag of terrestrial MORB and mantle lherzolites
350 (Figure 2), respectively, support the conclusions of limited fractionation of Ag and Cu at a
351 range of magmatic conditions, consistent with experimental data. These results suggest that
352 the Cu/Ag ratios in mantle rocks and their melting products should reflect the mantle
353 composition of a planetary body, regardless of the specific compositions and magmatic
354 evolution and regardless whether silicate magmas were saturated with a sulfide melt or not.

355 **4.3. Cu/Ag ratios in the Martian mantle and in bulk Mars**

356 **4.3.1. *The Ag content and Cu/Ag in the Martian mantle***

357 On the basis of variations in major and trace element and Sr-Nd-Os isotopic
358 compositions, the parent magmas of Martian meteorites were interpreted to originate from
359 incompatible element-depleted to enriched mantle sources and underwent different extents of
360 partial melting and fractional crystallization at different physiochemical conditions (e.g., Borg
361 and Draper, 2003; Brandon et al., 2012; Debaille et al., 2009; Herd et al., 2002; references
362 therein). It was also argued that Sr-Nd isotopic variations may reflect strong Martian crustal
363 contamination, particularly in enriched shergottites (Jones, 2015 and references therein).
364 Regardless of these complexities, the Cu/Ag ratios in different Martian meteorites are similar
365 within a factor of 2 and show no correlation with La/Yb ratios and initial $\epsilon^{143}\text{Nd}$ (Figure 3).
366 These observations suggest that the depletion and re-enrichment processes that resulted in
367 substantial variations of incompatible lithophile elements and their radiogenic isotopes led to
368 only a small and non-systematic variation of Cu/Ag in Martian mantle sources.

369 The limited variations in Martian meteorites yield a mean Cu/Ag of 1080 ± 320 (1s,
370 $n=14$, except ALH 84001). Because of sulfide-undersaturated conditions, both Cu and Ag
371 should enter silicate melts quantitatively after a few percent partial melting (Ding et al., 2015;
372 Wang and Becker, 2017), and thus, the mean ratio of the Martian meteorites is interpreted to
373 reflect that of the Martian mantle. Because the value is calculated from all shergottites and
374 nakhlites of this study, the uncertainty includes the possible effect of crustal contamination
375 and primordial heterogeneity of the mantle. Within uncertainty, the mean value is similar to
376 Cu/Ag of Y-980459 and LAR 06319, which were interpreted to have crystallized from

377 primitive mantle-derived magma (e.g., Basu Sarbadhikari et al., 2009; Mikouchi et al., 2004;
378 Musselwhite et al., 2006; Usui et al., 2012). The Cu content in the Martian mantle has been
379 estimated at 2.0 ± 0.4 $\mu\text{g/g}$ (1s) (Taylor, 2013; Wang and Becker, 2017), thus based on Cu/Ag,
380 the Ag content of the Martian mantle is 1.9 ± 0.7 ng/g (1s). The latter value overlaps with a
381 previous estimate of 2.6 ng/g Ag in the Martian mantle, which was estimated from Ag/La in a
382 limited set of Martian meteorites (Kong et al., 1999). Another recent estimate of the Ag
383 content of the Martian mantle was based on Ag/Dy and is twice as high (4.2 ± 1.2 ng/g , 1s,
384 Taylor, 2013).

385 **4.3.2. *The effect of core formation on Cu/Ag in planetary mantles***

386 The current Martian core-mantle boundary may be at a pressure of 20-23 GPa and a
387 temperature of about 2000 K (Fei and Bertka, 2005; Khan and Connolly, 2008; Konopliv et
388 al., 2011; Stewart et al., 2007). Data on metal-silicate partitioning experiments for a variety of
389 non-volatile siderophile elements such as W, Mo, Ni, Co, and the abundances of these
390 elements in model compositions of the Martian mantle suggest that the Martian mantle may
391 have equilibrated with the core at 14 ± 3 GPa and 2000-2300 K (Rai and van Westrenen, 2013;
392 Righter and Chabot, 2011; Yang et al., 2015).

393 Experimental studies have covered this P-T range for metal-silicate partitioning of Cu
394 and Ag and the influence of other parameters (Corgne et al., 2008; Righter, 2011; Righter and
395 Drake, 2000; Vogel, 2015; Wheeler et al., 2011; Wood et al., 2014). Silver and Cu become
396 less siderophile with increasing P and T and more siderophile with increasing S content in the
397 metal (Corgne et al., 2008; Vogel, 2015; Wood et al., 2014). In contrast, Si contents in the
398 metal and oxygen fugacity appear to have very weak effects (Vogel, 2015). Copper tends to

399 become slightly less siderophile with increasing oxygen fugacity (Corgne et al., 2008).
400 Remarkably, although the absolute partition coefficients may change dramatically with
401 variable conditions (a factor of tens or more), the relative siderophile behavior of Cu and Ag
402 changes little (Figure 5). For instance, metal-sulfide-silicate partitioning data from the same
403 experiments at 1.5 GPa and 1460-1650 °C (Wood et al., 2014) show only a factor of 1-3
404 variations, with a modest decrease in the ratios of exchange coefficients K_{Cu}/K_{Ag} (about 1.8 to
405 about 0.6, a mean of 1.2 ± 0.6 , 1s, n=10) from the metal-silicate system to the sulfide-silicate
406 system (Figure 5b). Data at higher P-T conditions (11-21 GPa, 2000-2600 °C, ΔIW of -4.7
407 to -1.6) also show limited fractionation of Cu and Ag, although Cu and Ag data are not from
408 the same experiments (Vogel, 2015). Therefore, experimental data predict that core formation
409 should have yielded low Cu and Ag abundances in the Martian mantle (as observed), but
410 should have had a limited effect on the Cu/Ag ratio of the mantle, compared to the bulk
411 planet.

412 Different domains of the Martian mantle are not homogenous and likely underwent
413 different extents of equilibration with the core, as indicated by ^{182}W isotopic heterogeneities
414 (e.g., Lee and Halliday, 1997). These heterogeneities preserve a memory of Hf-W
415 fractionations within the first 60 Ma since formation of the solar system, and indicate that the
416 early Martian mantle was not fully homogenized by convection and melting processes after
417 accretion and core formation were completed. We note that the Cu/Ag in different mantle
418 domains is similar (maximum difference by a factor of 2), reflecting the limited fractionation
419 of Cu and Ag during metal-silicate partitioning. Thus, as expected from data on partition

420 coefficients of Cu and Ag, incomplete core-mantle equilibration hardly affected Cu/Ag ratios
421 in the Martian mantle.

422 Besides metal-silicate segregation, it was also proposed that segregation of iron
423 sulfide melt into the core (“Hadean matte”) may have occurred during the final stages of core
424 formation of some planetary bodies. In case of Earth, this process is necessary to explain the
425 depletion of some siderophile elements in the mantle and possibly the isotopic variations of
426 some chalcophile elements such as Cu (e.g., Laurenz et al., 2016; O'Neill, 1991; Rubie et al.,
427 2016; Savage et al., 2015; Wood et al., 2008). However, due to the high FeO content of the
428 Martian mantle of 18 wt. % (Taylor, 2013), the sulfur content at sulfide saturation in Martian
429 magmas may be too high to facilitate exsolution of sulfide melt at high temperatures.
430 Experimental results at 5 GPa and 1600 °C indicated a required S content at saturation of
431 about 3000 µg/g S in melts with 14 wt.% FeO (Ding et al., 2014) and the S content could be
432 even higher for high FeO Martian magmas (e.g., Smythe et al., 2017). The Martian mantle
433 likely has a low S content of 360±120 µg/g (Wang and Becker, 2017), far lower than the
434 values of > 2000 µg/g at sulfide saturation for conditions of the Martian magma ocean at
435 14±3 GPa (Ding et al., 2014; Laurenz et al., 2016). Thus, considering the present state of
436 knowledge, an immiscible sulfide melt appears to be an unlikely ingredient during Martian
437 core formation and magma ocean evolution (Wang and Becker, 2017). Formation of the
438 Martian core by metal-silicate or sulfide melt-silicate segregation should have strongly
439 fractionated and depleted the HSE contents in the mantle (e.g., Laurenz et al., 2016; Mann et
440 al., 2012). However, the HSE and Os isotopes in many Martian meteorites display chondritic
441 or nearly chondritic ratios, thus, late accretion, very likely also occurred after core formation

442 on Mars (e.g., Brandon et al., 2012; Dale et al., 2012), although other workers proposed that
443 the HSE contents in the Martian mantle can be explained by core formation (Righter et al.,
444 2015). CI chondrite normalized Cu/Pd and Ag/Pd ratios are > 3 , indicating that the dominant
445 fraction of Cu and Ag in the Martian mantle was accreted during the main stages of accretion,
446 rather than by late accretion (Figure 6). Sulfide melt-silicate segregation would not have
447 affected the Cu/Ag ratios as variable S contents during metal-silicate or sulfide melt-silicate
448 partitioning of Cu and Ag hardly affected their relative behavior (Figure 5).

449 **4.3.3. Comparison of Cu/Ag ratios in Mars and chondrites**

450 Because metal-silicate and sulfide melt-silicate melt fractionation cause relatively
451 limited fractionation of Cu from Ag (within a factor of 3, Figure 5), we evaluate abundance
452 variations of Cu and Ag in primitive solar system objects, as such materials may represent
453 potential building materials of terrestrial planets. In Figure 4, we have compiled Cu and Ag
454 data of different groups of chondrites, including our new data. The compilation includes data
455 on samples for which both Cu and Ag contents are available (H, L, L/LL, LL chondrites: this
456 work, Friedrich et al., 2004; Friedrich et al., 2003; CI, CM, CV, CO chondrites: Friedrich et
457 al., 2002; Wang et al., 2015; and EH and EL chondrites: Kong et al., 1997; Wang and
458 Lipschutz, 2005). The mean Cu/Ag ratios of most groups of chondrites (CI, CM, CV, CO, H,
459 L, LL and EH) are similar (mean Cu/Ag = 1100 ± 400 , 1s, Wasson and Kallemeyn, 1988,
460 Figure 4) and close to the solar ratio of about 600 (Lodders, 2003).

461 The ordinary chondrites analyzed in this study are mostly falls, which show
462 negligible terrestrial contamination. The Cu/Ag ratios of these chondrites are within the range
463 of literature data on ordinary chondrites (Figure 4). Overall, ordinary chondrites show a larger

464 scatter of Cu/Ag ratios (ranging from 200 to 4500) than other chondrite classes. The larger
465 range in Cu/Ag is mainly due to the large variation in Ag contents (e.g., Friedrich et al., 2004;
466 Schönbächler et al., 2008; Schaefer and Fegley, 2010). Terrestrial contamination likely is not
467 the main reason of the scatter of Ag concentrations as the data obtained in this study on falls
468 show a similar scatter as literature data. A possible reason for the scatter of Ag abundances
469 may be impact-induced shock heating, which appears to mobilize Ag at higher shock intensity
470 (Friedrich et al., 2004) and thus only the data of ordinary chondrites with shock stages S1-3
471 (Friedrich et al., 2004) are shown in Figure 4. Parent body metamorphism of ordinary
472 chondrites also may have an effect on Ag contents as indicated by our new data and the
473 compiled data (Figure 1 in Schaefer and Fegley, 2010). Previous studies on Ag isotopes and
474 volatility calculations have suggested the possibility of volatility-controlled loss or
475 redistribution of Ag during open-system parent body thermal metamorphism (Schönbächler et
476 al., 2008; Schaefer and Fegley, 2010). The specific reasons for the larger variations of Ag
477 contents in ordinary chondrites relative to carbonaceous and enstatite chondrites need further
478 detailed work. Nevertheless, most ordinary chondrites (mean Cu/Ag = 1600 ± 1000 , 1s, n=39,
479 median = 1400) have Cu/Ag in the range of carbonaceous and enstatite chondrites (mean
480 Cu/Ag = 1100 ± 400 , 1s, n=24, median = 1000, Figure 4).

481 The similar mean Cu/Ag in different groups of chondrites (mean Cu/Ag = 1100 ± 400 ,
482 1s) indicates similar volatility of Cu and Ag in the different formation regions of these
483 chondrites in the solar nebula. The limited fractionation of Cu and Ag in chondrites is
484 consistent with the very similar condensation behavior of these elements in solar gas ($T_{50\%}$
485 near 1000 K at $P = 10^{-4}$ atm, Lodders, 2003). Recently, Kiseeva and Wood (2015) proposed

486 that Ag may have a significantly lower 50% condensation temperature ($T_{50\%}$ near 700 K)
487 compared to previous estimates, assuming that Ag should condense mainly into FeS, whereas
488 Cu ($T_{50\%}$ near 1000 K) condenses into metal and FeS. Enstatite chondrites and carbonaceous
489 chondrites contain different proportions of metal and sulfides. For instance, EH chondrites are
490 enriched in metal and sulfides relative to most other chondrites and the proportions of metal
491 to sulfides vary widely in carbonaceous chondrites. The similar Cu/Ag ratios in different
492 groups of enstatite and carbonaceous chondrites are inconsistent with a different condensation
493 behavior of Cu and Ag. The similarity of Cu/Ag ratios in the majority of chondrites may
494 imply only a small range of Cu/Ag ratios in the building materials of terrestrial planets. The
495 Cu/Ag ratio of the Martian mantle (1080 ± 320 , 1s) is indistinguishable from the majority of
496 chondrites (except some ordinary chondrites) and only slightly higher than the ratio of about
497 600 in CI chondrites. This observation thus is consistent with models that Mars was built
498 from materials with chondritic Cu/Ag ratios and with a limited change in Cu/Ag during
499 Martian metal-silicate segregation (at most a factor of 2).

500 To conclude, Martian core formation has led to low Cu and Ag contents in the mantle,
501 but likely with little change of Cu/Ag, which thus retained a value indistinguishable from
502 most chondrites. This conclusion is consistent with available metal-sulfide-silicate
503 partitioning experimental data (Figure 5). Consequently, the mean Cu/Ag of Martian
504 meteorites reflects the ratio of the mantle and of bulk Mars. Given the less than a factor of 2
505 change in the relative siderophile and chalcophile behavior of Cu and Ag at different core
506 formation and magmatic conditions, this conclusion should be robust and applicable to other
507 planetary bodies, at least for those with a size equivalent to Mars or smaller.

508 **4.4. Comparison between the mantles of Mars and Earth**

509 The late stages of metal-silicate and sulfide-silicate segregation during the formation
510 of Earth's core is now believed to have taken place at very high P-T conditions (presumably
511 $P > 40$ GPa and $T > 2300^{\circ}\text{C}$), which requires extrapolation of partition coefficients from
512 available experimental conditions (e.g., Fischer et al., 2015; Mann et al., 2009; Rubie et al.,
513 2015; Rubie et al., 2016; Siebert et al., 2011; Wade and Wood, 2005). Comparison of Cu/Ag
514 ratios in the mantles of Mars and Earth might reveal the effects of low ($< 2000^{\circ}\text{C}$ and
515 corresponding pressures near the liquidus curve of the mantle) vs. high P-T core formation on
516 Cu and Ag concentrations and on Cu/Ag in planetary mantles. Mars and Earth likely accreted
517 from different proportions of primitive material of variable composition as differences in their
518 $\Delta^{17}\text{O}$ suggest (Franchi et al., 1999; Lodders and Fegley, 1997). These planets also underwent
519 different accretion and core formation histories, because Mars is smaller than Earth and the
520 Martian core likely formed much earlier than Earth (Kleine et al., 2004; Kleine et al., 2009;
521 Lee and Halliday, 1997; Righter, 2011; Righter and Chabot, 2011; Righter et al., 1998; Rubie
522 et al., 2011; Rubie et al., 2004; Wade and Wood, 2005; Yang et al., 2015). Here we will
523 discuss how these differences affect the relative depletion of Cu and Ag and Cu/Ag ratios in
524 the mantles of Mars and Earth.

525 The Cu contents in the mantles of both Mars and Earth are lower than in chondrites
526 which show a predominant range of 80-200 $\mu\text{g/g}$ Cu (Figure 4). The Cu and Ag contents in
527 the Martian mantle are lower than in the Earth's mantle, by a factor of 15 for Cu and of 4-5
528 for Ag (Figure 6). The Martian mantle seems to have somewhat higher abundances of
529 lithophile volatile elements (e.g., K, Rb) compared to Earth's mantle, as K/U and Rb/Sr data

530 show (Dreibus and Wänke, 1985; Halliday et al., 2001, Figure 6). Data on other lithophile to
531 weakly siderophile elements such as Zn (Wang et al., 2016 and references therein) support
532 this view (e.g., Lodders and Fegley, 1997). This difference is commonly interpreted to
533 indicate that bulk Mars is somewhat less depleted in volatile elements (compared to CI
534 chondrites) than the Earth (e.g., Dreibus and Wänke, 1985).

535 If we conservatively assume that Mars is at least similarly depleted in moderately
536 volatile elements as Earth, the larger depletion of Cu and Ag in the Martian mantle must be a
537 consequence of core formation. Both Ag and Cu become less siderophile with increasing P
538 and T and many core formation models have explained the depletion of Cu in the mantle of
539 Earth and Mars by metal segregation (Corgne et al., 2008; Righter, 2011; Righter and Drake,
540 2000; Vogel, 2015; Wood et al., 2014; Yang et al., 2015). The greater depletion of Cu and Ag
541 in the Martian mantle is consistent with the partitioning behavior of Cu and Ag at lower P-T
542 core formation conditions because Mars' mass is equivalent to only about 1/10 of the Earth's
543 mass. Figure 7 is a simple illustration of the changes of metal-metal oxide exchange
544 coefficients $K_D(\text{Cu-Fe})$ and Cu contents in the silicate mantle of an Earth-size body during
545 accretion. The curves in Figure 7 are based on the parameterization of $K_D(\text{Cu-Fe})$ with P-T
546 (Corgne et al., 2008) and a single-stage equilibrium core formation model with a mean Cu
547 content of 100 $\mu\text{g/g}$ assumed for accreted materials. Given the limited variation of Cu
548 contents in different chondrites, a somewhat different Cu content would not change the result
549 significantly. Other factors such as light element abundances in the metal and the details of
550 accretion processes also affect $K_D(\text{Cu-Fe})$ and the Cu content in the mantle, thus Figure 7 is
551 schematic for the overall evolution of $K_D(\text{Cu-Fe})$ and Cu abundances as a function of the size

552 of the body (i.e., P-T), provided metal and silicates predominantly equilibrate during
553 accretion (Note the purpose is not to explain the specific Cu contents in the mantles of Mars
554 and Earth, but to show the trend of $K_D(\text{Cu-Fe})$ with increasing P-T). Because the function of
555 Corgne et al. (2008) is based on P-T conditions far lower than those believed to be relevant
556 for the formation of Earth's core, the extrapolation of $K_D(\text{Cu-Fe})$ to very high P-T conditions
557 may have a large uncertainty.

558 As shown for the case of Mars, core formation on small planetary bodies leads to a
559 strong depletion of Cu and Ag in the silicate fraction because of high $K_D(\text{Cu-Fe})$ at low P-T
560 conditions (Figure 7). For example, Cu in the Martian mantle is depleted by a factor of
561 50-100 relative to chondrites (Figure 4). During accretion of larger terrestrial planets such as
562 Earth (i.e., higher mean P-T of core formation), $K_D(\text{Cu-Fe})$ tends to decrease, thus leading to
563 a higher Cu content in the mantle (e.g., Corgne et al., 2008; Righter, 2011; Righter and Drake,
564 2000; Vogel, 2015; Yang et al., 2015). It follows that the contents of moderately siderophile
565 Cu and Ag in Earth's mantle mainly reflect the late stage history of accretion and core
566 formation when the proto-Earth already accreted most of its mass. The actual accretion
567 history of volatile elements is difficult to assess. The abundances of Cu and Ag are consistent
568 with suggestions that more volatile-rich material was accreted during the final high P-T stage
569 of Earth's main accretion phase (e.g., Rubie et al., 2011; Schönbächler et al., 2010; Wade and
570 Wood, 2005). However, accretion of volatile-rich material is also possible during the early
571 stages of Earth's accretion (e.g., Rubie et al., 2015).

572 During accretion, a fraction of metallic cores of differentiated bodies may not
573 equilibrate with the mantle and directly merge during collisions (Halliday, 2004; Jacobsen

574 and Harper, 1996; Rubie et al., 2011). Disequilibrium metal-silicate segregation would
575 preserve the effects of low P-T metal-silicate partitioning from smaller differentiated bodies.
576 The high Cu and Ag contents in the Earth's mantle indicate high extents of
577 metal-sulfide-silicate equilibration during late terrestrial core formation (e.g., Rudge et al.,
578 2010), otherwise, the Earth's mantle would contain much less Cu and Ag.

579 In comparison to the large differences in the depletion factor of Cu in the mantles of
580 Mars and Earth relative to CI chondrites (a factor of 50-100 and 3-6, respectively), the Cu/Ag
581 ratios in the mantles show only a small difference, e.g., 1080 ± 320 in the Martian mantle
582 (similar to most chondrites) and 3500 ± 1000 in the Earth's mantle (Figure 4). The factor of 3
583 higher Cu/Ag in Earth's mantle reflects either metal-sulfide-silicate equilibration during core
584 formation at very high P-T conditions or, a nonchondritic composition of Earth's building
585 materials, or volatility-controlled processes such as preferential volatilization of Ag during
586 giant impacts. Given the limited variations of Cu/Ag in different groups of chondrites (Figure
587 4) and the reported effects of impact-induced shock heating on Ag (Friedrich et al., 2004), the
588 non-chondritic Cu/Ag of Earth more likely reflects fractionation of Cu/Ag during high P-T
589 core formation and possible volatile element loss during giant impacts. Because Ag is slightly
590 more chalcophile than Cu during high P-T sulfide-silicate partitioning relative to
591 metal-silicate partitioning (K_{Cu}/K_{Ag} show about a factor of 3 variation with a mean of $1.2 \pm$
592 0.6 , Figure 5b), late segregation of sulfide matte into Earth's core may have removed slightly
593 more Ag and led to the higher Cu/Ag in Earth's mantle. However, it should be noted that the
594 behavior of chalcophile elements in liquids and gases at extreme P-T conditions, as might be
595 relevant for the final stages of accretion of Earth, is still quite uncertain.

5. Conclusions

596

597 This study has presented Ag contents obtained by isotope dilution ICP-MS and
598 Cu/Ag ratios in shergottites and nakhlites and new data on ordinary chondrites. The parent
599 magmas of the Martian meteorites originated from different mantle sources and underwent
600 different magmatic evolution, but display a limited variation in Cu/Ag ratios (1080 ± 320 , 1s,
601 $n=14$). The new results and data from terrestrial mantle rocks and mantle-derived magmas
602 indicate limited fractionation of Cu from Ag during high temperature magmatic evolution at
603 variable physicochemical conditions as experimentally determined sulfide melt-silicate melt
604 partitioning data predict, regardless whether sulfide saturation was reached or not. Thus, the
605 relatively constant Cu/Ag value in the Martian meteorites likely is representative of the
606 Martian mantle, and based on Cu/Ag, the Ag content of the Martian mantle is estimated at
607 1.9 ± 0.7 ng/g (1s).

608 The low concentrations of Cu and Ag in the Martian mantle are in contrast to the
609 relatively high abundances of lithophile volatile elements and indicate that Cu and Ag were
610 controlled by core formation. The very different concentrations of Cu and Ag in the Martian
611 and in Earth's mantle support the notion that the partitioning of some siderophile and
612 chalcophile elements during planetary core formation scales with the size of the planetary
613 body, which is particularly important for the differentiation of large terrestrial planets such as
614 Earth. Experimental studies of metal-silicate segregation at low- and high P-T conditions
615 indicate that core formation may lead to no or at most only a moderate ($< \text{factor } 3$) increase of
616 Cu/Ag in mantle compositions, compared to bulk planet compositions. The Cu/Ag in the
617 Martian mantle is indistinguishable from values in most chondrites, indicating no significant

618 fractionation of this ratio during core formation on Mars. The Cu/Ag ratio in the Martian
619 mantle thus reflects that of bulk Mars. The Cu/Ag of Earth's mantle is a factor of 2-3 higher
620 than in most chondrites and in the Martian mantle, which may reflect the effects of very high
621 P-T core formation and/or segregation of sulfide matte into Earth's core. Alternative
622 explanations include a slightly non-chondritic volatile element composition of Earth's
623 building materials (Wang et al., 2016), or volatility-controlled loss of Ag during accretion of
624 Earth. These explanations are considered less likely given the relatively high abundances of
625 Cu and Ag in Earth's mantle, which are consistent with results from high-P-T experimental
626 studies.

627

628 **Acknowledgements:** We acknowledge support by the providers of Martian meteorites and
629 chondrites (Meteorite Working Group, ANSMET and the National Museum of Natural
630 History, Smithsonian Institution, USNM, USA; Antarctic Meteorite Research Center, NIPR,
631 Japan; C. Smith, Natural History Museum London, UK; J. Zipfel, Senckenberg Institute,
632 Frankfurt am Main, Germany). We thank M. Feth, O. Jaeger and P. Gleissner for help and
633 support in the laboratory and C. Li and E. Hoffmann for discussion. This work was supported
634 by DFG funding (Be1820/12-1 and SFB-TRR 170 Subproject B1). This is SFB-TRR 170
635 Publication No. 9. We thank associate guest editor Marc-Alban Millet and Jung-Woo Park
636 and Kate Kiseeva for constructive comments.

637

638

639 **Figure caption**

640

641 Figure 1. Silver contents versus MgO and Cu contents in Martian meteorites. a) Ag contents
642 in shergottites from the present study show a broadly negative correlation with MgO contents.
643 b) Ag and Cu contents show a positive correlation for data of the present study. The Ag data
644 of this study are similar to or lower than literature values (Table 2). The difference may
645 reflect the large analytical uncertainty of the previously applied methods or sample
646 heterogeneity. Literature data were obtained by INAA and RNAA (Biswas et al., 1980; Kong
647 et al., 1999; Laul et al., 1986; Lodders, 1998; Smith et al., 1984; Treiman et al., 1986; Wang
648 et al., 1998) or laser ablation-ICP-MS (Yang et al., 2015). The Cu data on samples from the
649 present study are from Wang and Becker (2017). The bulk circle represents the value of the
650 Martian mantle, and the Ag content is 1.9 ± 0.7 ng/g (1s, see Section 4.3.1) and Cu of 2.0 ± 0.4
651 $\mu\text{g/g}$ (1s) (Taylor, 2013; Wang and Becker, 2017). Note that the Ag values on Figure 1a are
652 cut off at the value of 40 and there are many higher values (see Figure 1b), and due to scale
653 ALH84001 is not shown in Figure 1b.

654

655

656 Figure 2. Cu/Ag ratios versus MgO contents in different groups of Martian meteorites,
657 terrestrial MORB, Hawaiian basalts and peridotites. In the basaltic (green triangle),
658 olivine-phyric (yellow triangle) and lherzolitic (purple triangle) shergottites and nakhlites (red
659 square), Cu/Ag ratios overall are similar and reflect the Martian mantle (blue band). Most
660 terrestrial peridotites (3500 ± 1200 , 1s, $n=38$, for fresh peridotites with $\text{Al}_2\text{O}_3 \geq 2$ wt.%,

661 Wang and Becker, 2015) show Cu/Ag ratios similar to global MORB glasses (3600 ± 400 , 1s,
662 $n=338$, Jenner and O'Neill, 2012), MORB sulfide droplets (Cu/Ag = 3000 ± 300 , 1s, $n=7$, gray
663 band, Patten et al., 2013). Due to Ag enrichment during terrestrial alteration, some peridotites
664 have lower Cu/Ag contents at given MgO contents (see details in Wang and Becker, 2015).
665 Mantle-derived magmatic rocks on Mars and Earth formed at different physicochemical
666 conditions, but the Cu/Ag ratios in these rocks are relatively constant on Mars and Earth,
667 respectively. Data sources for the mantle contents of MgO and Cu/Ag: the Earth's mantle
668 (Palme and O'Neill, 2014; Wang and Becker, 2015) and the Martian mantle (Taylor, 2013;
669 this study).

670

671 Figure 3. Cu/Ag versus CI chondrite normalized La/Yb ratio (a) and initial $\epsilon^{143}\text{Nd}$ (b). The
672 La/Yb data (Lodders, 2003; Meyer, 2013) and initial $\epsilon^{143}\text{Nd}$ (Debaille et al., 2009; Jones,
673 2015; Shih et al., 2014; Shih et al., 2005; Shih et al., 1999; Shirai and Ebihara, 2009;
674 references therein) are from the literature. The lithophile incompatible element tracers display
675 no systematic variation with Cu/Ag.

676

677 Figure 4. The Cu/Ag ratios in the mantles of Mars and Earth and in different groups of
678 chondrites. Mars shows a strong depletion of Cu (and Ag, not shown) in the mantle relative to
679 chondrites (a factor of 50-100). In contrast, the depletion of Cu is much smaller for the
680 Earth's mantle (a factor of 3-5). However, Cu/Ag ratios in the mantle of Mars and Earth do
681 not show such a large difference as the concentrations (only a factor of 3). Carbonaceous
682 chondrites and EH chondrites have similar Cu/Ag ratios and overlap with ordinary chondrites,

683 which show a larger scatter. Data on chondrites with both Cu and Ag data on the same sample
684 are indicated by small symbol sizes (H, L, LL: Friedrich et al., 2004; Friedrich et al., 2003;
685 this study; CI, CM, CV, CO: Friedrich et al., 2002; Wang et al., 2015; EH and EL: Kong et al.,
686 1997; Wang and Lipschutz, 2005). The mean Cu/Ag of different groups of chondrites (H, L,
687 LL, EH, EL, CI, CM, CO and CV indicated by larger symbols than those of the individual
688 samples) are calculated from the average Cu and Ag contents of the groups (Wasson and
689 Kallemeyn, 1988). See details in the text.

690

691 Figure 5. Compiled metal-metal oxide exchange coefficients (K_D relative to Fe) and partition
692 coefficients (D , based on mass fraction) of Cu and Ag in experimental metal-sulfide-silicate
693 systems. a-b, Cu and Ag are moderately siderophile and become less siderophile with
694 increasing P-T, but more siderophile with increasing S content in the metal (Vogel, 2015;
695 Wood et al., 2014). Copper and Ag display limited fractionation in metal-sulfide-silicate
696 systems (K_{DCu}/K_{DAg} with a mean of 1.2 ± 0.6 , 1s, n=10, b). The relative partitioning behavior
697 of Cu and Ag appears to slightly change from sulfide-poor to sulfur-rich metals (b). c-d,
698 during sulfide melt-silicate melt partitioning, partition coefficients $D_{Cu}^{sulfide/silicate\ melt}$ and
699 $D_{Ag}^{sulfide/silicate\ melt}$ change dramatically as a function of changing compositions, e.g., FeO
700 content in silicate melts; whereas the relative partition coefficients of Cu and Ag change little
701 (Kiseeva and Wood, 2013; Kiseeva and Wood, 2015; Li and Audetat, 2012). Experimental
702 data of Kiseeva and Wood (2013, 2015) were obtained at 1.5 GPa and a range of temperatures
703 (1300-1700°C) and Cu- and Ni- contents of sulfides, whereas experiments of the study of Li
704 and Audetat (2012) were conducted at 1.5-3.0 GPa and 1175-1300°C.

705

706 Figure 6. CI chondrite and Mg normalized contents of representative lithophile (in gray) and
707 siderophile (in color) elements in the mantles of Mars (circle) and Earth (triangle). Note that
708 abundances of moderately volatile elements in bulk Mars are higher than in bulk Earth as is
709 indicated by the abundances of lithophile volatile elements (a). Panel b highlights the HSE,
710 Cu, Ag, S, Se and Te in panel a, emphasizing the effect of P-T on Cu and Ag during core
711 formation. Data sources: CI chondrite (Lodders, 2003); Earth's mantle (Becker et al., 2006;
712 Palme and O'Neill, 2014; Wang and Becker, 2013, 2015); Martian mantle (this study; Taylor,
713 2013; Wang and Becker, 2017; Yang et al., 2015).

714

715 Figure 7. Schematic illustration of the evolution of the exchange coefficient K_D (Cu-Fe)
716 between iron metal and silicate melts and Cu content in the mantle of a planetary body with
717 increasing pressure-temperature during accretion. The main purpose is to show the effect of
718 increasing P-T (Corgne et al., 2008). The large value of K_D (Cu-Fe) indicates a very low Cu
719 content in the silicate mantle after core formation at low P-T (e.g., at Mars-size or smaller).
720 At high P-T conditions, Cu becomes less siderophile and thus leads to a higher Cu content in
721 the mantle. Because the function used here (Corgne et al., 2008) is based on P-T conditions
722 far lower than those of the likely formation of Earth's core, the extrapolation of K_D (Cu-Fe) to
723 very high P-T conditions may have large uncertainty (dashed trends shown). Because of the
724 similar behavior of Cu and Ag (Figure 5), this may also apply to Ag.

725

726

727

6. References

- 728 Alard, O., Griffin, W.L., Lorand, J.P., Jackson, S.E. and O'Reilly, S.Y. (2000) Non-chondritic
729 distribution of the highly siderophile elements in mantle sulphides. *Nature* 407, 891-894.
- 730 Balta, J.B., McSween, H.Y., Tucker, K. and Wadhwa, M. (2015) Petrology and Geochemistry
731 of New Antarctic Shergottites: LAR 12011, LAR 12095, and LAR 12240. 46th Lunar and
732 Planetary Science Conference, Contribution No. 1832, p.2294.
- 733 Basu Sarbadhikari, A., Day, J.M.D., Liu, Y., Rumble Iii, D. and Taylor, L.A. (2009)
734 Petrogenesis of olivine-phyric shergottite Larkman Nunatak 06319: Implications for enriched
735 components in martian basalts. *Geochim. Cosmochim. Acta* 73, 2190-2214.
- 736 Becker, H., Horan, M.F., Walker, R.J., Gao, S., Lorand, J.-P. and Rudnick, R.L. (2006)
737 Highly siderophile element composition of the Earth's primitive upper mantle: Constraints
738 from new data on peridotite massifs and xenoliths. *Geochim. Cosmochim. Acta* 70,
739 4528-4550.
- 740 Biswas, S., Ngo, H.T. and Lipschutz, M.E. (1980) Trace element contents of selected
741 Antarctic meteorites. I. Weathering effects and ALH A77005, A77257, A77278 and A77299.
742 *Zeitschrift für Naturforschung A* 35, 191-196.
- 743 Bockrath, C., Ballhaus, C. and Holzheid, A. (2004) Fractionation of the Platinum-Group
744 Elements During Mantle Melting. *Science* 305, 1951-1953.
- 745 Borg, L.E. and Draper, D.S. (2003) A petrogenetic model for the origin and compositional
746 variation of the martian basaltic meteorites. *Meteorit. Planet. Sci.* 38, 1713-1731.
- 747 Brandon, A.D., Puchtel, I.S., Walker, R.J., Day, J.M.D., Irving, A.J. and Taylor, L.A. (2012)
748 Evolution of the martian mantle inferred from the (187)Re-(187)Os isotope and highly
749 siderophile element abundance systematics of shergottite meteorites. *Geochim. Cosmochim.*
750 *Acta* 76, 206-235.
- 751 Canup, R.M., Visscher, C., Salmon, J. and Fegley Jr, B. (2015) Lunar volatile depletion due
752 to incomplete accretion within an impact-generated disk. *Nat. Geosci.* 8, 918-921.
- 753 Chevrier, V., Lorand, J.-P. and Sautter, V. (2011) Sulfide petrology of four nakhlites:
754 Northwest Africa 817, Northwest Africa 998, Nakhla, and Governador Valadares. *Meteorit.*
755 *Planet. Sci.* 46, 769-784.
- 756 Corgne, A., Keshav, S., Wood, B.J., McDonough, W.F. and Fei, Y.W. (2008) Metal-silicate
757 partitioning and constraints on core composition and oxygen fugacity during Earth accretion.
758 *Geochim. Cosmochim. Acta* 72, 574-589.

- 759 Czamanske, G.K. and Moore, J.G. (1977) Composition and phase chemistry of sulfide
760 globules in basalt from the Mid-Atlantic Ridge rift valley near 37°N lat. *Geol. Soc. Am. Bull.*
761 88, 587-599.
- 762 Dale, C.W., Burton, K.W., Greenwood, R.C., Gannoun, A., Wade, J., Wood, B.J. and Pearson,
763 D.G. (2012) Late Accretion on the Earliest Planetesimals Revealed by the Highly Siderophile
764 Elements. *Science* 336, 72-75.
- 765 Davis, A.M. (2006) Volatile Evolution and Loss, in: Jr., D.S.L.a.H.Y.M. (Ed.), *Meteorites*
766 *and the Early Solar System II*. University of Arizona Press, Tucson, pp. 295-307.
- 767 Dare, S., Barnes, S.-J., Prichard, H. and Fisher, P. (2011) Chalcophile and platinum-group
768 element (PGE) concentrations in the sulfide minerals from the McCreeley East deposit,
769 Sudbury, Canada, and the origin of PGE in pyrite. *Mineral. Deposita* 46, 381-407.
- 770 Dauphas, N. and Pourmand, A. (2015) Thulium anomalies and rare earth element patterns in
771 meteorites and Earth: Nebular fractionation and the nugget effect. *Geochim. Cosmochim.*
772 *Acta* 163, 234-261.
- 773 Dauphas, N. (2017) The isotopic nature of the Earth's accreting material through time. *Nature*
774 541, 521-524.
775
- 776 Debaille, V., Brandon, A.D., O'Neill, C., Yin, Q.Z. and Jacobsen, B. (2009) Early martian
777 mantle overturn inferred from isotopic composition of nakhlite meteorites. *Nat. Geosci.* 2,
778 548-552.
- 779 Ding, S., Dasgupta, R., Lee, C.-T.A. and Wadhwa, M. (2015) New bulk sulfur measurements
780 of Martian meteorites and modeling the fate of sulfur during melting and crystallization –
781 Implications for sulfur transfer from Martian mantle to crust–atmosphere system. *Earth Planet.*
782 *Sci. Lett.* 409, 157-167.
- 783 Ding, S., Dasgupta, R. and Tsuno, K. (2014) Sulfur concentration of martian basalts at sulfide
784 saturation at high pressures and temperatures – Implications for deep sulfur cycle on Mars.
785 *Geochim. Cosmochim. Acta* 131, 227-246.
- 786 Dreibus, G. and Wänke, H. (1985) Mars, a Volatile-Rich Planet. *Meteoritics* 20, 367-381.
- 787 Farquhar, J., Savarino, J., Jackson, T.L. and Thiemens, M.H. (2000) Evidence of atmospheric
788 sulphur in the martian regolith from sulphur isotopes in meteorites. *Nature* 404, 50-52.
- 789 Fei, Y. and Bertka, C. (2005) The Interior of Mars. *Science* 308, 1120-1121.
- 790 Fellows, S.A. and Canil, D. (2012) Experimental study of the partitioning of Cu during partial
791 melting of Earth's mantle. *Earth Planet. Sci. Lett.* 337–338, 133-143.

792 Fischer, R.A., Nakajima, Y., Campbell, A.J., Frost, D.J., Harries, D., Langenhorst, F.,
793 Miyajima, N., Pollok, K. and Rubie, D.C. (2015) High pressure metal–silicate partitioning of
794 Ni, Co, V, Cr, Si, and O. *Geochim. Cosmochim. Acta* 167, 177-194.

795 Franchi, I.A., Wright, I.P., Sexton, A.S. and Pillinger, C.T. (1999) The oxygen-isotopic
796 composition of Earth and Mars. *Meteorit. Planet. Sci.* 34, 657-661.

797 Franz, H.B., Kim, S.-T., Farquhar, J., Day, J.M.D., Economos, R.C., McKeegan, K.D.,
798 Schmitt, A.K., Irving, A.J., Hoek, J. and Iii, J.D. (2014) Isotopic links between atmospheric
799 chemistry and the deep sulphur cycle on Mars. *Nature* 508, 364-368.

800 Friedrich, J.M., Bridges, J.C., Wang, M.S. and Lipschutz, M.E. (2004) Chemical studies of L
801 chondrites. VI: Variations with petrographic type and shock-loading among equilibrated falls.
802 *Geochim. Cosmochim. Acta* 68, 2889-2904.

803 Friedrich, J.M., Wang, M.S. and Lipschutz, M.E. (2002) Comparison of the trace element
804 composition of Tagish Lake with other primitive carbonaceous chondrites. *Meteorit. Planet.*
805 *Sci.* 37, 677-686.

806 Friedrich, J.M., Wang, M.S. and Lipschutz, M.E. (2003) Chemical studies of L chondrites. V:
807 Compositional patterns for 49 trace elements in 14 L4-6 and 7 LL4-6 falls. *Geochim.*
808 *Cosmochim. Acta* 67, 2467-2479.

809 Fortin, M.-A., Riddle, J., Desjardins-Langlais, Y. and Baker, D.R. (2015) The effect of water
810 on the sulfur concentration at sulfide saturation (SCSS) in natural melts. *Geochim.*
811 *Cosmochim. Acta* 160, 100-116.

812 Greenwood, J.P., Mojzsis, S.J. and Coath, C.D. (2000) Sulfur isotopic compositions of
813 individual sulfides in Martian meteorites ALH84001 and Nakhla: implications for
814 crust–regolith exchange on Mars. *Earth Planet. Sci. Lett.* 184, 23-35.

815 Halliday, A.N. (2004) Mixing, volatile loss and compositional change during impact-driven
816 accretion of the Earth. *Nature* 427, 505-509.

817 Halliday, A.N., Wanke, H., Birck, J.L. and Clayton, R.N. (2001) The accretion, composition
818 and early differentiation of Mars. *Space Science Reviews* 96, 197-230.

819 Herd, C.D.K., Borg, L.E., Jones, J.H. and Papike, J.J. (2002) Oxygen fugacity and
820 geochemical variations in the martian basalts: implications for martian basalt petrogenesis and
821 the oxidation state of the upper mantle of Mars. *Geochim. Cosmochim. Acta* 66, 2025-2036.

822 Herd, C., Duke, M., Bryden, C. and Pearson, D. (2013) Tissint among the shergottites:
823 Parental melt composition, redox state, La/Yb and V/Sc, Lunar and Planetary Science
824 Conference, p. 2683.

- 825 Jacobsen, S.B. and Harper, C.L. (1996) Accretion and early differentiation history of the
826 Earth based on extinct radionuclides, *Earth Processes: Reading the Isotopic Code*. American
827 Geophysical Union, pp. 47-74.
- 828 Jenner, F.E. and O'Neill, H.S.C. (2012) Analysis of 60 elements in 616 ocean floor basaltic
829 glasses. *Geochem. Geophys. Geosyst.* 13, Q02005, doi:02010.01029/02011GC004009.
- 830 Jenner, F.E., O'Neill, H.S.C., Arculus, R.J. and Mavrogenes, J.A. (2010) The magnetite crisis
831 in the evolution of arc-related magmas and the initial concentration of Au, Ag and Cu. *J.*
832 *Petrol.* 51, 2445-2464.
- 833 Jones, J.H. (2015) Various aspects of the petrogenesis of the Martian shergottite meteorites.
834 *Meteorit. Planet. Sci.* 50, 674-690.
- 835 Jones, J.H. and Drake, M.J. (1986) Geochemical constraints on core formation in the Earth.
836 *Nature* 322, 221-228.
- 837 Jones, J.H., Neal, C.R. and Ely, J.C. (2003) Signatures of the highly siderophile elements in
838 the SNC meteorites and Mars: a review and petrologic synthesis. *Chem. Geol.* 196, 21-41.
- 839 Kaczaral, P.W., Dodd, R.T. and Lipschutz, M.E. (1989) Chemical studies of L chondrites: IV.
840 Antarctic/non-Antarctic comparisons. *Geochim. Cosmochim. Acta* 53, 491-501.
- 841 Kadlag, Y. and Becker, H. (2015) Fractionation of highly siderophile and chalcogen elements
842 in components of EH3 chondrites. *Geochim. Cosmochim. Acta* 161, 166-187.
- 843 Khan, A. and Connolly, J.A.D. (2008) Constraining the composition and thermal state of
844 Mars from inversion of geophysical data. *Journal of Geophysical Research: Planets* 113,
845 E07003.
- 846 Kiseeva, E.S. and Wood, B.J. (2013) A simple model for chalcophile element partitioning
847 between sulphide and silicate liquids with geochemical applications. *Earth Planet. Sci. Lett.*
848 383, 68-81.
- 849 Kiseeva, E.S. and Wood, B.J. (2015) The effects of composition and temperature on
850 chalcophile and lithophile element partitioning into magmatic sulphides. *Earth Planet. Sci.*
851 *Lett.* 424, 280-294.
- 852 Kleine, T., Mezger, K., Munker, C., Palme, H. and Bischoff, A. (2004) Hf-182-W-182
853 isotope systematics of chondrites, eucrites, and martian meteorites: Chronology of core
854 formation and early mantle differentiation in Vesta and Mars. *Geochim. Cosmochim. Acta* 68,
855 2935-2946.
- 856 Kleine, T., Touboul, M., Bourdon, B., Nimmo, F., Mezger, K., Palme, H., Jacobsen, S.B., Yin,
857 Q.Z. and Halliday, A.N. (2009) Hf-W chronology of the accretion and early evolution of
858 asteroids and terrestrial planets. *Geochim. Cosmochim. Acta* 73, 5150-5188.

- 859 Koblitz, J. (2005) MetBase 7.2 for Microsoft Windows™ : The meteorite data retrieval
860 software and bibliography on meteoritics and planetary science.
- 861 Kong, P., Ebihara, M. and Palme, H. (1999) Siderophile elements in Martian meteorites and
862 implications for core formation in Mars. *Geochim. Cosmochim. Acta* 63, 1865-1875.
- 863 Kong, P., Mori, T. and Ebihara, M. (1997) Compositional continuity of enstatite chondrites
864 and implications for heterogeneous accretion of the enstatite chondrite parent body. *Geochim.*
865 *Cosmochim. Acta* 61, 4895-4914.
- 866 Konopliv, A.S., Asmar, S.W., Folkner, W.M., Karatekin, Ö., Nunes, D.C., Smrekar, S.E.,
867 Yoder, C.F. and Zuber, M.T. (2011) Mars high resolution gravity fields from MRO, Mars
868 seasonal gravity, and other dynamical parameters. *Icarus* 211, 401-428.
- 869 Lapen, T.J., Richter, M., Brandon, A.D., Debaille, V., Beard, B.L., Shafer, J.T. and Peslier,
870 A.H. (2010) A Younger Age for ALH84001 and Its Geochemical Link to Shergottite Sources
871 in Mars. *Science* 328, 347-351.
- 872 Laul, J.C., Keays, R.R., Ganapathy, R., Anders, E. and Morgan, J.W. (1972) Chemical
873 fractionations in meteorites—V. Volatile and siderophile elements in achondrites and ocean
874 ridge basalts. *Geochim. Cosmochim. Acta* 36, 329-345.
- 875 Laul, J.C., Smith, M.R., Wänke, H., Jagoutz, E., Dreibus, G., Palme, H., Spettel, B., Burghele,
876 A., Lipschutz, M.E. and Verkouteren, R.M. (1986) Chemical systematics of the shergotty
877 meteorite and the composition of its parent body (Mars). *Geochim. Cosmochim. Acta* 50,
878 909-926.
- 879 Laurenz, V., Rubie, D.C., Frost, D.J. and Vogel, A.K. (2016) The importance of sulfur for the
880 behaviour of highly-siderophile elements during Earth's differentiation. *Geochim.*
881 *Cosmochim. Acta* 194, 123-138.
- 882 Lee, D.C. and Halliday, A.N. (1997) Core formation on Mars and differentiated asteroids.
883 *Nature* 388, 854-857.
- 884 Lee, C.-T.A., Luffi, P., Chin, E.J., Bouchet, R., Dasgupta, R., Morton, D.M., Le Roux, V.,
885 Yin, Q.-z. and Jin, D. (2012) Copper Systematics in Arc Magmas and Implications for
886 Crust-Mantle Differentiation. *Science* 336, 64-68.
- 887 Li, J. and Agee, C.B. (1996) Geochemistry of mantle-core differentiation at high pressure.
888 *Nature* 381, 686-689.
- 889 Li, J. and Agee, C.B. (2001) The effect of pressure, temperature, oxygen fugacity and
890 composition on partitioning of nickel and cobalt between liquid Fe-Ni-S alloy and liquid
891 silicate: implications for the earth's core formation. *Geochim. Cosmochim. Acta* 65,
892 1821-1832.

- 893 Li, Y. and Audetat, A. (2012) Partitioning of V, Mn, Co, Ni, Cu, Zn, As, Mo, Ag, Sn, Sb, W,
894 Au, Pb, and Bi between sulfide phases and hydrous basanite melt at upper mantle conditions.
895 *Earth Planet. Sci. Lett.* 355, 327-340.
- 896 Lingner, D.W., Huston, T.J., Hutson, M. and Lipschutz, M.E. (1987) Chemical studies of H
897 chondrites. I: Mobile trace elements and gas retention ages. *Geochim. Cosmochim. Acta* 51,
898 727-739.
- 899 Liu, Y., Samaha, N.-T. and Baker, D.R. (2007) Sulfur concentration at sulfide saturation
900 (SCSS) in magmatic silicate melts. *Geochim. Cosmochim. Acta* 71, 1783-1799.
- 901 Liu, X., Xiong, X., Aud  tat, A., Li, Y., Song, M., Li, L., Sun, W. and Ding, X. (2014)
902 Partitioning of copper between olivine, orthopyroxene, clinopyroxene, spinel, garnet and
903 silicate melts at upper mantle conditions. *Geochim. Cosmochim. Acta* 125, 1-22.
904
- 905 Lodders, K. (1998) A survey of shergottite, nakhlite and chassigny meteorites whole-rock
906 compositions. *Meteorit. Planet. Sci.* 33, A183-A190.
- 907 Lodders, K. (2003) Solar system abundances and condensation temperatures of the elements.
908 *Astrophys. J.* 591, 1220-1247.
- 909 Lodders, K. and Fegley, B. (1997) An oxygen isotope model for the composition of Mars.
910 *Icarus* 126, 373-394.
- 911 Lorand, J.P. (1989) Abundance and distribution of Cu-Fe-Ni sulfides, sulfur, copper and
912 platinum-group elements in orogenic-type spinel lherzolite massifs of Ari  ge (northeastern
913 Pyrenees, France). *Earth Planet. Sci. Lett.* 93, 50-64.
- 914 Lorand, J.P., Chevrier, V. and Sautter, V. (2005) Sulfide mineralogy and redox conditions in
915 some shergottites. *Meteorit. Planet. Sci.* 40, 1257-1272.
- 916 Lugu  t, A., Lorand, J.P., Alard, O. and Cottin, J.Y. (2004) A multi-technique study of
917 platinum group element systematic in some Ligurian ophiolitic peridotites, Italy. *Chem. Geol.*
918 208, 175-194.
- 919 Mann, U., Frost, D.J. and Rubie, D.C. (2009) Evidence for high-pressure core-mantle
920 differentiation from the metal-silicate partitioning of lithophile and weakly-siderophile
921 elements. *Geochim. Cosmochim. Acta* 73, 7360-7386.
- 922 Mann, U., Frost, D.J., Rubie, D.C., Becker, H. and Audetat, A. (2012) Partitioning of Ru, Rh,
923 Pd, Re, Ir and Pt between liquid metal and silicate at high pressures and high temperatures -
924 Implications for the origin of highly siderophile element concentrations in the Earth's mantle.
925 *Geochim. Cosmochim. Acta* 84, 593-613.
- 926 McCubbin, F.M., Riner, M.A., Vander Kaaden, K.E. and Burkemper, L.K. (2012) Is Mercury
927 a volatile-rich planet? *Geophys. Res. Lett.* 39, Doi:10.1029/2012GL051711.

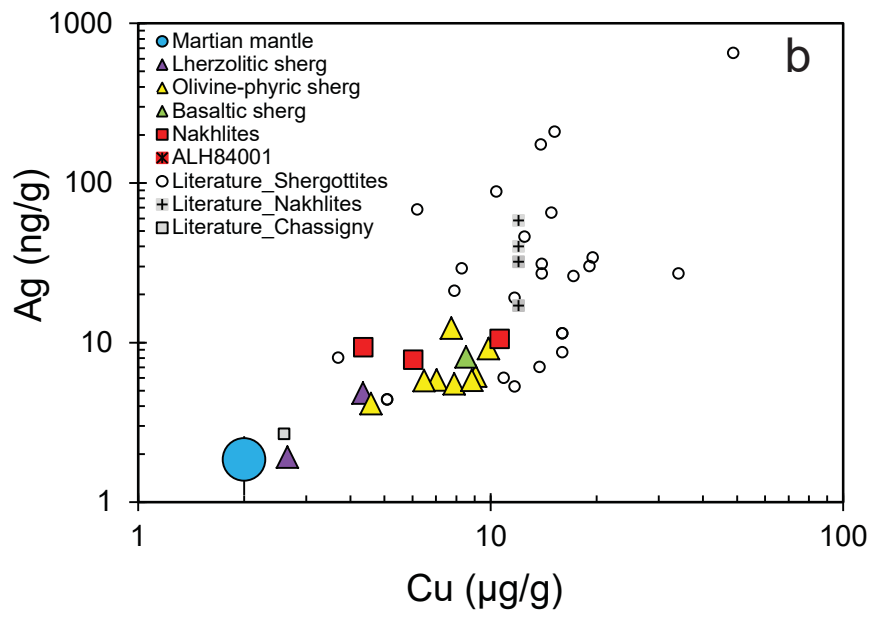
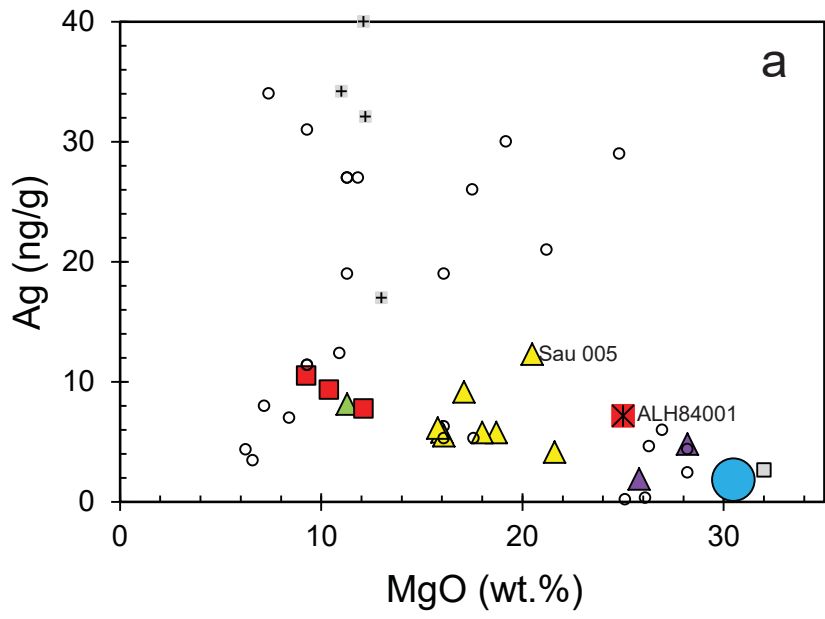
- 928 McDonough, W.F. (2014) 3.16 - Compositional Model for the Earth's Core, in: Holland, H.D.,
929 Turekian, K.K. (Eds.), *Treatise on Geochemistry (Second Edition)*. Elsevier, Oxford, pp.
930 559-577.
- 931 Meyer, C. (2013) *The Martian Meteorite Compendium*. Astromaterials Research &
932 Exploration Science (ARES), <http://curator.jsc.nasa.gov/antmet/mmc/>.
- 933 Mikouchi, T., Koizumi, E., McKay, G., Monkawa, A., Ueda, Y., Chokai, J. and Miyamoto, M.
934 (2004) Yamato 980459: mineralogy and petrology of a new shergottite-related rock from
935 Antarctica. *Antarctic meteorite research* 17, 13.
- 936 Mittlefehldt, D.W. (1994) ALH84001, a cumulate orthopyroxenite member of the martian
937 meteorite clan. *Meteoritics* 29, 214-221.
- 938 Musselwhite, D.S., Dalton, H.A., Kiefer, W.S. and Treiman, A.H. (2006) Experimental
939 petrology of the basaltic shergottite Yamato-980459: Implications for the thermal structure of
940 the Martian mantle. *Meteorit. Planet. Sci.* 41, 1271-1290.
- 941 Nittler, L.R., Starr, R.D., Weider, S.Z., McCoy, T.J., Boynton, W.V., Ebel, D.S., Ernst, C.M.,
942 Evans, L.G., Goldsten, J.O., Hamara, D.K., Lawrence, D.J., McNutt, R.L., Schlemm, C.E.,
943 Solomon, S.C. and Sprague, A.L. (2011) The Major-Element Composition of Mercury's
944 Surface from MESSENGER X-ray Spectrometry. *Science* 333, 1847-1850.
- 945 Nyquist, L.E., Bogard, D.D., Shih, C.Y., Greshake, A., Stoffler, D. and Eugster, O. (2001)
946 Ages and geologic histories of Martian meteorites. *Space Science Reviews* 96, 105-164.
- 947 O'Neill, H.S.C. (1991) The origin of the moon and the early history of the earth—A chemical
948 model. Part 2: The earth. *Geochim. Cosmochim. Acta* 55, 1159-1172.
- 949 Palme, H. and O'Neill, H.S.C. (2014) 3.1 - Cosmochemical Estimates of Mantle Composition,
950 in: Holland, H.D., Turekian, K.K. (Eds.), *Treatise on Geochemistry (Second Edition)*.
951 Elsevier, Oxford, pp. 1-39.
- 952 Patten, C., Barnes, S.-J., Mathez, E.A. and Jenner, F.E. (2013) Partition coefficients of
953 chalcophile elements between sulfide and silicate melts and the early crystallization history of
954 sulfide liquid: LA-ICP-MS analysis of MORB sulfide droplets. *Chem. Geol.* 358, 170-188.
- 955 Peplowski, P.N., Evans, L.G., Hauck, S.A., McCoy, T.J., Boynton, W.V., Gillis-Davis, J.J.,
956 Ebel, D.S., Goldsten, J.O., Hamara, D.K., Lawrence, D.J., McNutt, R.L., Nittler, L.R.,
957 Solomon, S.C., Rhodes, E.A., Sprague, A.L., Starr, R.D. and Stockstill-Cahill, K.R. (2011)
958 Radioactive Elements on Mercury's Surface from MESSENGER: Implications for the Planet's
959 Formation and Evolution. *Science* 333, 1850-1852.
- 960 Rai, N. and van Westrenen, W. (2013) Core-mantle differentiation in Mars. *Journal of*
961 *Geophysical Research-Planets* 118, 1195-1203.

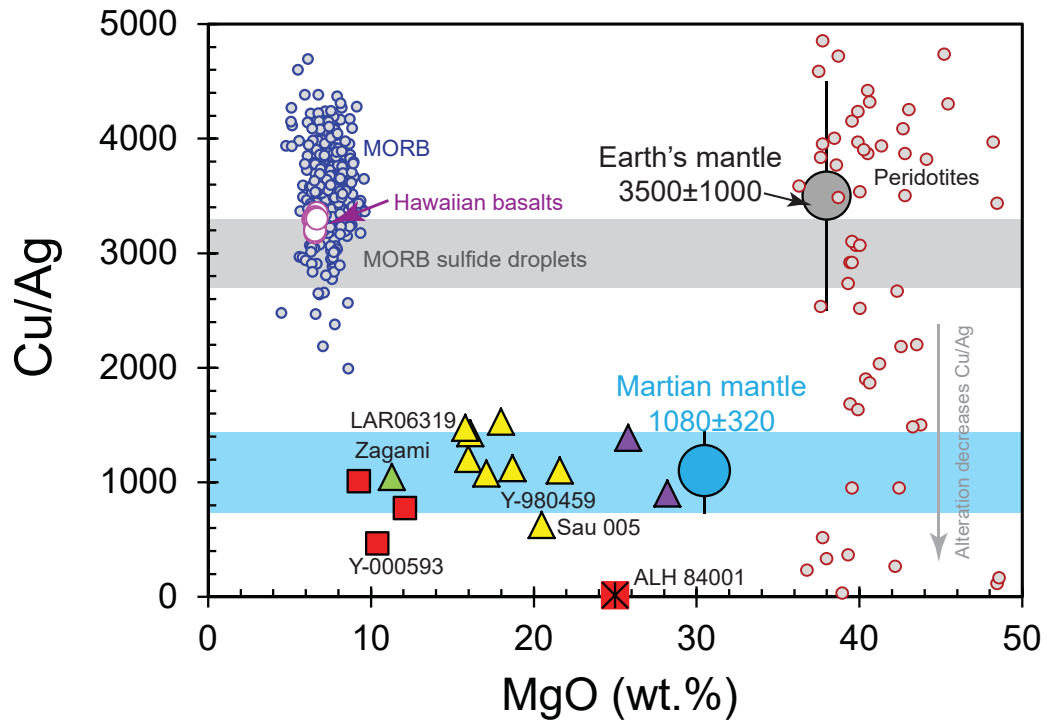
- 962 Righter, K. (2011) Prediction of metal-silicate partition coefficients for siderophile elements:
963 An update and assessment of PT conditions for metal-silicate equilibrium during accretion of
964 the Earth. *Earth Planet. Sci. Lett.* 304, 158-167.
- 965 Righter, K. and Chabot, N.L. (2011) Moderately and slightly siderophile element constraints
966 on the depth and extent of melting in early Mars. *Meteorit. Planet. Sci.* 46, 157-176.
- 967 Righter, K., Danielson, L.R., Pando, K.M., Williams, J., Humayun, M., Hervig, R.L. and
968 Sharp, T.G. (2015) Highly siderophile element (HSE) abundances in the mantle of Mars are
969 due to core formation at high pressure and temperature. *Meteorit. Planet. Sci.* 50, 604-631.
- 970 Righter, K. and Drake, M.J. (2000) Metal/silicate equilibrium in the early Earth—New
971 constraints from the volatile moderately siderophile elements Ga, Cu, P, and Sn. *Geochim.*
972 *Cosmochim. Acta* 64, 3581-3597.
- 973 Righter, K., Hervig, R.L. and Kring, D.A. (1998) Accretion and core formation on Mars:
974 Molybdenum contents of melt inclusion glasses in three SNC meteorites. *Geochim.*
975 *Cosmochim. Acta* 62, 2167-2177.
- 976 Righter, K., Pando, K. and Danielson, L.R. (2009) Experimental evidence for sulfur-rich
977 martian magmas: Implications for volcanism and surficial sulfur sources. *Earth Planet. Sci.*
978 *Lett.* 288, 235-243.
- 979 Rubie, D.C., Frost, D.J., Mann, U., Asahara, Y., Nimmo, F., Tsuno, K., Kegler, P., Holzheid,
980 A. and Palme, H. (2011) Heterogeneous accretion, composition and core-mantle
981 differentiation of the Earth. *Earth Planet. Sci. Lett.* 301, 31-42.
- 982 Rubie, D.C., Gessmann, C.K. and Frost, D.J. (2004) Partitioning of oxygen during core
983 formation on the Earth and Mars. *Nature* 429, 58-61.
- 984 Rubie, D.C., Jacobson, S.A., Morbidelli, A., O'Brien, D.P., Young, E.D., de Vries, J., Nimmo,
985 F., Palme, H. and Frost, D.J. (2015) Accretion and differentiation of the terrestrial planets
986 with implications for the compositions of early-formed Solar System bodies and accretion of
987 water. *Icarus* 248, 89-108.
- 988 Rubie, D.C., Laurenz, V., Jacobson, S.A., Morbidelli, A., Palme, H., Vogel, A.K. and Frost,
989 D.J. (2016) Highly siderophile elements were stripped from Earth's mantle by iron sulfide
990 segregation. *Science* 353, 1141-1144.
- 991 Rudge, J.F., Kleine, T. and Bourdon, B. (2010) Broad bounds on Earth's accretion and core
992 formation constrained by geochemical models. *Nat. Geosci.* 3, 439-443.
- 993 Savage, P.S., Moynier, F., Chen, H., Shofner, G., Siebert, J., Badro, J. and Puchtel, I.S. (2015)
994 Copper isotope evidence for large-scale sulphide fractionation during Earth's differentiation.
995 *Geochemical Perspectives Letters* 1, 53-64.

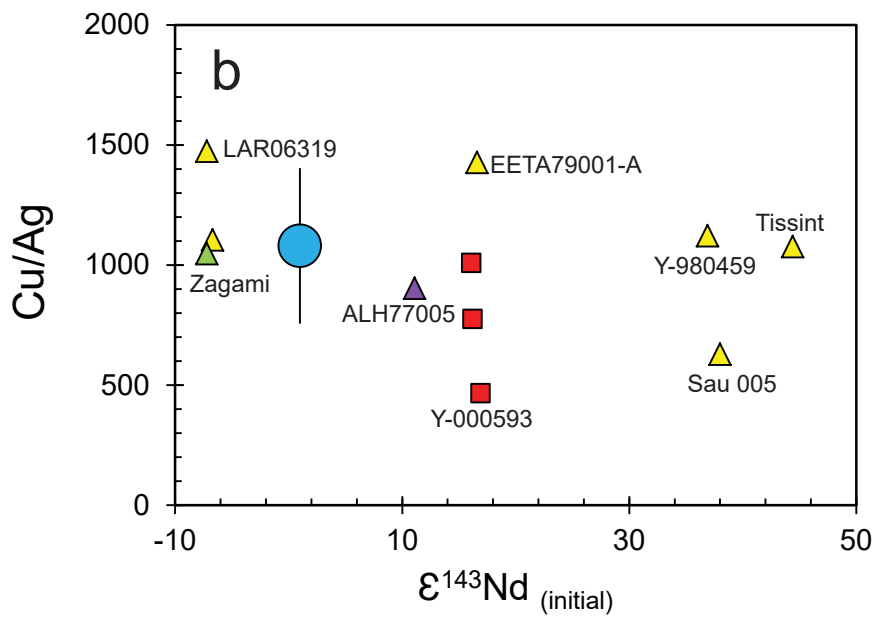
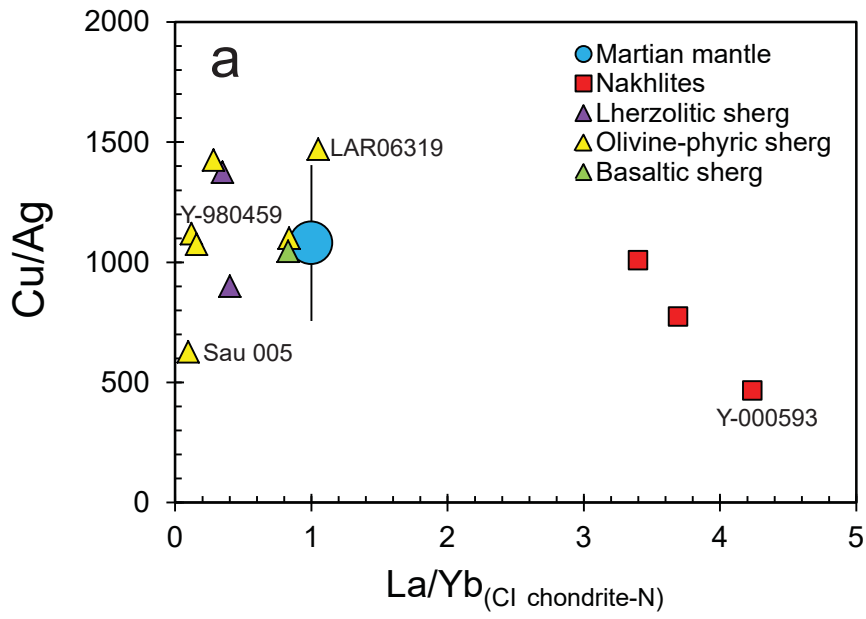
- 996 Schönbacher, M., Carlson, R.W., Horan, M.F., Mock, T.D. and Hauri, E.H. (2008) Silver
997 isotope variations in chondrites: Volatile depletion and the initial ^{107}Pd abundance of the
998 solar system. *Geochim. Cosmochim. Acta* 72, 5330-5341.
- 999 Schönbacher, M., Carlson, R.W., Horan, M.F., Mock, T.D. and Hauri, E.H. (2010)
1000 Heterogeneous accretion and the moderately volatile element budget of Earth. *Science* 328,
1001 884-887.
- 1002 Schaefer, L. and Fegley, B. (2010) Volatile element chemistry during metamorphism of
1003 ordinary chondritic material and some of its implications for the composition of asteroids.
1004 *Icarus* 205, 483-496.
- 1005 Shih, C.-Y., Nyquist, L., Park, J. and Agee, C.B. (2014) Sm-Nd and Rb-Sr Isotopic
1006 Systematics of a Heavily Shocked Martian Meteorite Tissint and Petrogenesis of Depleted
1007 Shergottites. *Lunar and Planetary Science Conference* 45th.
- 1008 Shih, C.-Y., Nyquist, L.E., Wiesmann, H., Reese, Y. and Misawa, K. (2005) Rb-Sr and
1009 Sm-Nd dating of olivine-phyric shergottite Yamato 980459: Petrogenesis of depleted
1010 shergottites. *Antarctic meteorite research* 18, 46.
- 1011 Shih, C.Y., Nyquist, L.E. and Wiesmann, H. (1999) Samarium-neodymium and
1012 rubidium-strontium systematics of nakhlite Governador Valadares. *Meteorit. Planet. Sci.* 34,
1013 647-655.
- 1014 Shirai, N. and Ebihara, M. (2009) Chemical characteristics of the lherzolitic shergottite
1015 Yamato 000097: magmatism on Mars inferred from the chemical compositions of shergottites.
1016 *Polar Science* 3, 117-133.
- 1017 Siebert, J., Corgne, A. and Ryerson, F.J. (2011) Systematics of metal-silicate partitioning for
1018 many siderophile elements applied to Earth's core formation. *Geochim. Cosmochim. Acta* 75,
1019 1451-1489.
- 1020 Smith, M.R., Laul, J.C., Ma, M.S., Huston, T., Verkouteren, R.M., Lipschutz, M.E. and
1021 Schmitt, R.A. (1984) Petrogenesis of the SNC (shergottites, nakhlites, chassignites)
1022 meteorites: Implications for their origin from a large dynamic planet, possibly Mars. *Journal*
1023 *of Geophysical Research: Solid Earth* 89, B612-B630.
- 1024 Smythe, D., Wood, B. and Kiseeva, E. (2017) The S content of silicate melts at sulfide
1025 saturation: New experiments and a model incorporating the effects of sulfide composition.
1026 *Am. Mineral.* 102, 795-803.
- 1027 Stewart, A.J., Schmidt, M.W., van Westrenen, W. and Liebske, C. (2007) Mars: A new
1028 core-crystallization regime. *Science* 316, 1323-1325.
- 1029 Taylor, G.J. (2013) The bulk composition of Mars. *Chem. Erde Geochem.* 73, 401-420.

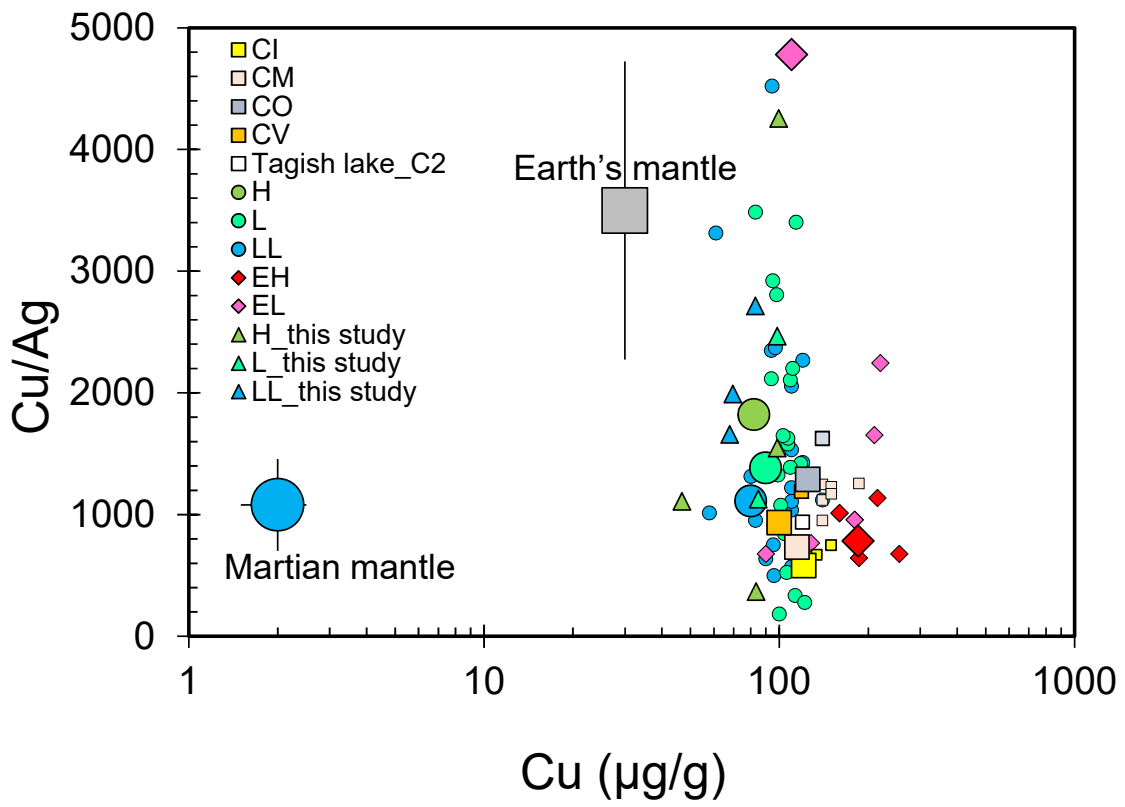
- 1030 Theis, K.J., Schonbachler, M., Benedix, G.K., Rehkamper, M., Andreasen, R. and Davies, C.
1031 (2013) Palladium-silver chronology of IAB iron meteorites. *Earth Planet. Sci. Lett.* 361,
1032 402-411.
- 1033 Treiman, A.H. (2005) The nakhlite meteorites: Augite-rich igneous rocks from Mars. *Chem.*
1034 *Erde-Geochem.* 65, 203-270.
- 1035 Treiman, A.H., Drake, M.J., Janssens, M.J., Wolf, R. and Ebihara, M. (1986) Core Formation
1036 in the Earth and Shergottite Parent Body (Spb) - Chemical Evidence from Basalts. *Geochim.*
1037 *Cosmochim. Acta* 50, 1071-1091.
- 1038 Usui, T., Alexander, C.M.O.D., Wang, J., Simon, J.I. and Jones, J.H. (2012) Origin of water
1039 and mantle–crust interactions on Mars inferred from hydrogen isotopes and volatile element
1040 abundances of olivine-hosted melt inclusions of primitive shergottites. *Earth Planet. Sci. Lett.*
1041 357–358, 119-129.
- 1042 Vogel, A.K. (2015) Siderophile element partitioning at high pressures and temperatures:
1043 Implications for core formation processes, Faculty of Biology, Chemistry and Earth Sciences.
1044 Universität Bayreuth, Bayreuth, p. 226.
- 1045 Wade, J. and Wood, B.J. (2005) Core formation and the oxidation state of the Earth. *Earth*
1046 *Planet. Sci. Lett.* 236, 78-95.
- 1047 Wadhwa, M. (2008) Redox Conditions on Small Bodies, the Moon and Mars. *Rev. Mineral.*
1048 *Geochem.* 68, 493-510.
- 1049 Wang, K. and Jacobsen, S.B. (2016) Potassium isotopic evidence for a high-energy giant
1050 impact origin of the Moon. *Nature* 538, 487-490.
- 1051 Wang, M.S. and Lipschutz, M.E. (2005) Thermal metamorphism of primitive meteorites - XII.
1052 The enstatite chondrites revisited. *Environmental Chemistry* 2, 215-226.
- 1053 Wang, M.S., Mokoš, J.A. and Lipschutz, M.E. (1998) Martian meteorites: Volatile trace
1054 elements and cluster analysis. *Meteorit. Planet. Sci.* 33, 671-675.
- 1055 Wang, Z. and Becker, H. (2013) Ratios of S, Se and Te in the silicate Earth require a
1056 volatile-rich late veneer. *Nature* 499, 328-331.
- 1057 Wang, Z. and Becker, H. (2015) Abundances of Ag and Cu in mantle peridotites and the
1058 implications for the behavior of chalcophile elements in the mantle. *Geochim. Cosmochim.*
1059 *Acta* 160, 209-226.
- 1060 Wang, Z. and Becker, H. (2017) Chalcophile elements in Martian meteorites indicate low
1061 sulfur content in the Martian interior and a volatile element-depleted late veneer. *Earth Planet.*
1062 *Sci. Lett.* 463, 56-68.
- 1063

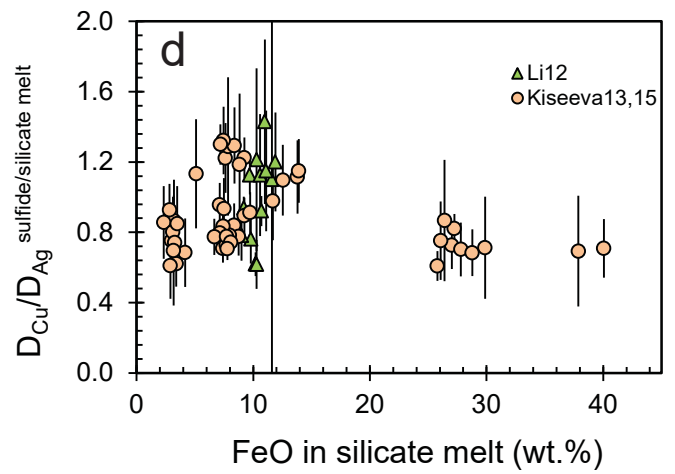
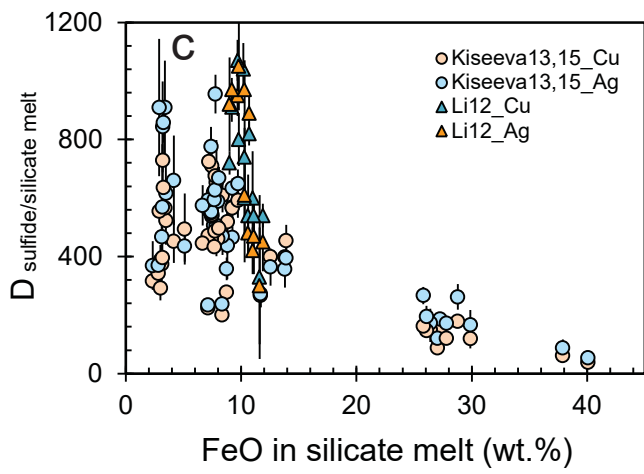
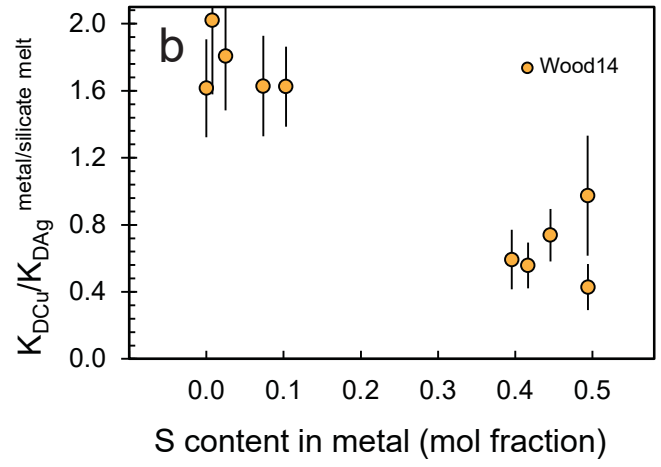
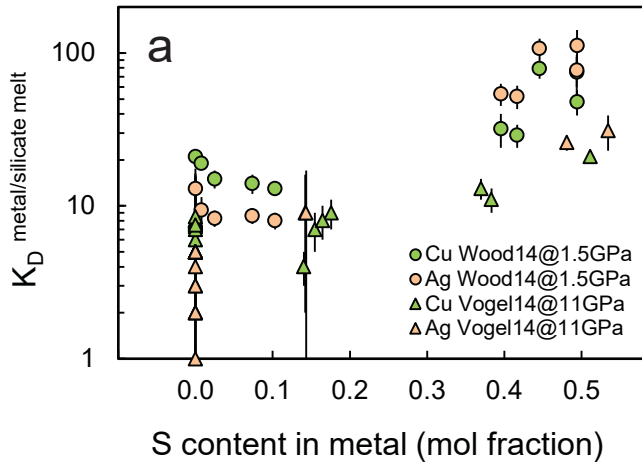
- 1064 Wang, Z., Becker, H. and Wombacher, F. (2015) Mass Fractions of S, Cu, Se, Mo, Ag, Cd, In,
1065 Te, Ba, Sm, W, Tl and Bi in Geological Reference Materials and Selected Carbonaceous
1066 Chondrites Determined by Isotope Dilution ICP-MS. *Geostand. Geoanal. Res.* 39, 185-208.
- 1067 Wang, Z., Laurenz, V., Petitgirard, S. and Becker, H. (2016) Earth's moderately volatile
1068 element composition may not be chondritic: Evidence from In, Cd and Zn. *Earth Planet. Sci.*
1069 *Lett.* 435, 136-146.
- 1070 Wasson, J.T. and Kallemeyn, G.W. (1988) Compositions of Chondrites. *Phil. Trans. R. Soc.*
1071 *A* 325, 535-544.
- 1072 Wheeler, K.T., Walker, D. and McDonough, W.F. (2011) Pd and Ag metal-silicate
1073 partitioning applied to Earth differentiation and core-mantle exchange. *Meteorit. Planet. Sci.*
1074 46, 199-217.
- 1075 Wolf, S.F. and Lipschutz, M.E. (1995) Chemical Studies of H Chondrites .6. Antarctic
1076 Non-Antarctic Composition Differences Revisited. *J. Geophys. Res.-Planets* 100, 3335-3349.
- 1077 Wolf, S.F., Wang, M.S., Dodd, R.T. and Lipschutz, M.E. (1997) Chemical studies of H
1078 chondrites .8. On contemporary meteoroid streams. *J. Geophys. Res.-Planets* 102, 9273-9288.
- 1079 Wood, B.J. (2008) Accretion and core formation: constraints from metal-silicate partitioning.
1080 *Philos. T. Roy. Soc. A* 366, 4339-4355.
- 1081 Wood, B.J. and Kiseeva, E.S. (2015) Trace element partitioning into sulfide: How lithophile
1082 elements become chalcophile and vice versa. *Am. Mineral.* 100, 2371-2379.
- 1083 Wood, B.J., Kiseeva, E.S. and Mirolo, F.J. (2014) Accretion and core formation: the effects
1084 of sulfur on metal-silicate partition coefficients. *Geochim. Cosmochim. Acta* 145, 248-267.
- 1085 Wood, B.J., Nielsen, S.G., Rehkamper, M. and Halliday, A.N. (2008) The effects of core
1086 formation on the Pb- and Tl- isotopic composition of the silicate Earth. *Earth Planet. Sci. Lett.*
1087 269, 325-335.
- 1088 Yang, S., Humayun, M., Righter, K., Jefferson, G., Fields, D. and Irving, A.J. (2015)
1089 Siderophile and chalcophile element abundances in shergottites: Implications for Martian core
1090 formation. *Meteorit. Planet. Sci.* 50, 691-714.

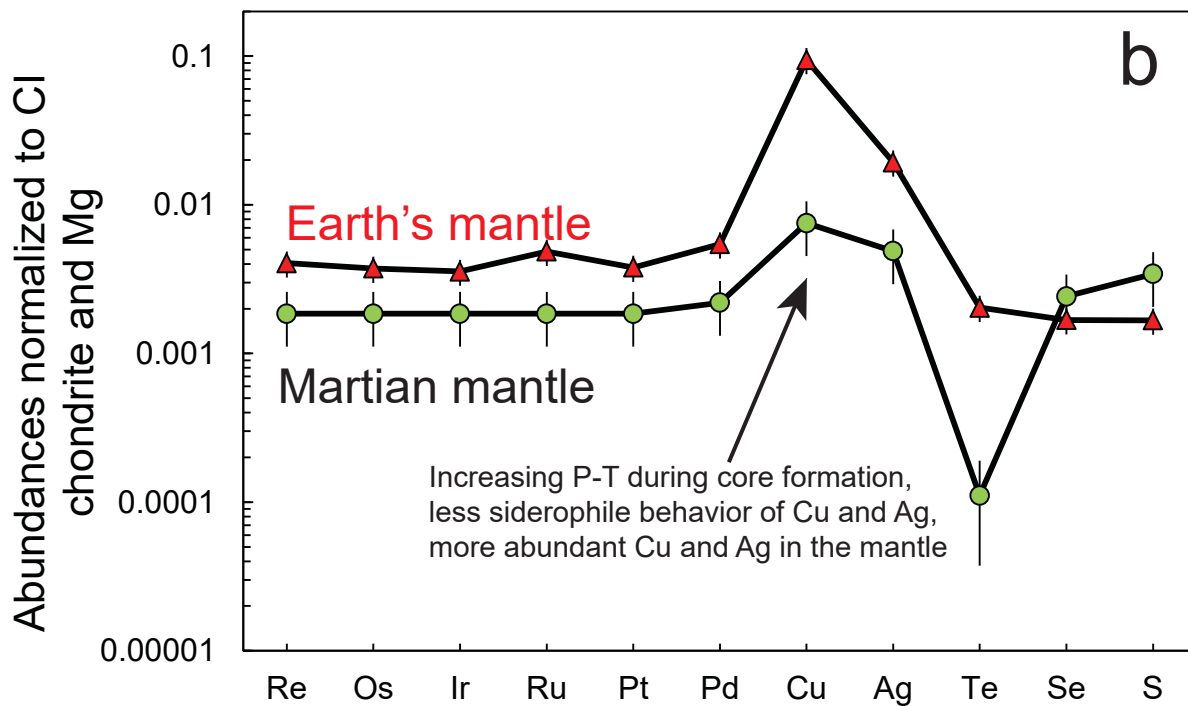
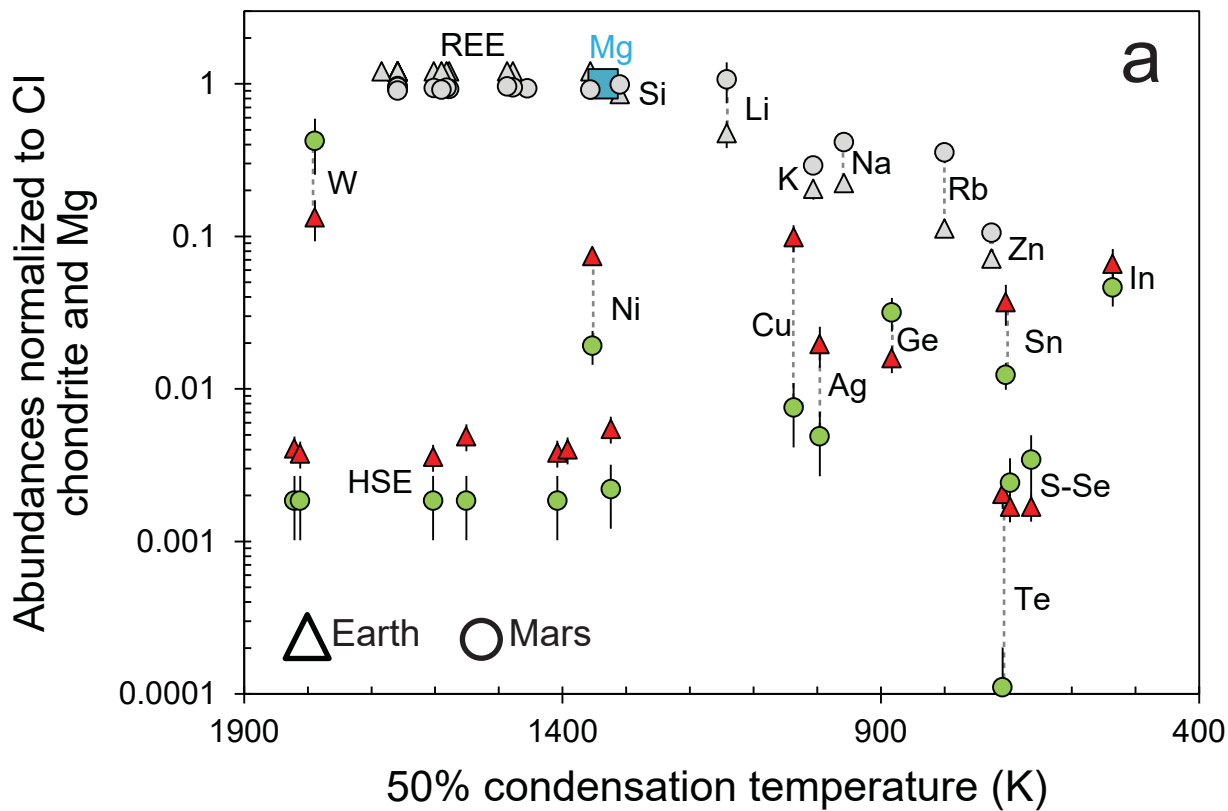












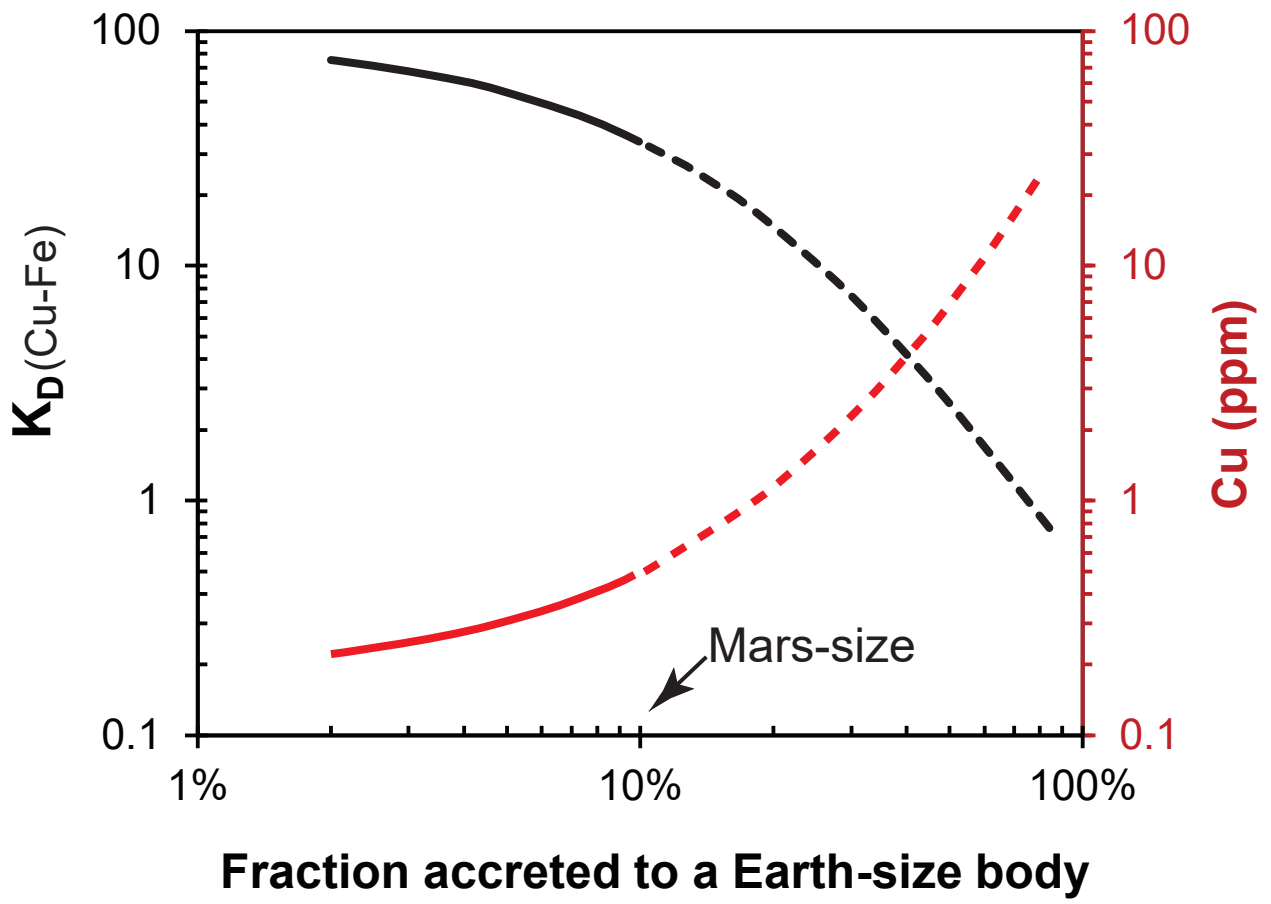


Table 1. Silver and Cu contents in Martian meteorites and other compositional information.

Sample Name	Institution	Inventory number	Fall/Find	Classification	Chemical features	Mass (g)	MgO	SiO ₂	Al ₂ O ₃	FeO	CaO	La/Yb _(CI-N)	ε ¹⁴³ Nd _(initial)	Ag			Cu*		Cu/Ag	
							(wt.%)	(wt.%)	(wt.%)	(wt.%)	(wt.%)	(ng/g)	±2s	Blank%	(μg/g)	±2s		±2s		
ALHA77005	ANSMET	248, 82 (Specific, Parent)	Antarctica	Lherzolithic shergottite	Intermediate	0.1284	28.2	42.4	2.9	20.1	3.2	0.40	11.1	4.8	0.2	4%	4.35	0.09	903	35
Y-000097	AMRC	87	Antarctica	Lherzolithic shergottite		0.1386	25.8	45.6	2.2	19.9	4.2	0.35		1.9	0.1	8%	2.65	0.04	1386	103
Sau 005	SM	MPI 1522/3	Hot desert	Olivine-phyric shergottite	Depleted	0.0946	20.5	47.2	4.5	18.3	5.7	0.10	38.0	12.3	0.2	2%	7.74	0.09	628	14
Y-980459	AMRC	77	Antarctica	Olivine-phyric shergottite	Depleted	0.1378	18.7	49.9	5.2	17.3	6.8	0.12	36.9	5.8	0.2	3%	6.49	0.06	1122	31
Tissint	NHML	off BM.2012, M3	Fall	Olivine-phyric shergottite	Depleted	0.1471	17.1	46.2	4.9	21.2	6.5	0.16	44.4	9.2	0.2	2%	9.87	0.09	1077	21
EETA 79001-A	ANSMET	209, 22 (Specific, Parent)	Antarctica	Olivine-phyric shergottite	Intermediate	0.1873	16.1	49.9	5.9	18.4	7.3	0.28	16.6	5.5	0.1	2%	7.88	0.07	1428	33
LAR 06319	ANSMET	67, 3 (Specific, Parent)	Antarctica	Olivine-phyric shergottite	Enriched	0.1357	15.8	46.7	6.0	20.4	6.5	1.05	-7.2	6.2	0.2	3%	9.07	0.18	1474	48
LAR 12011	ANSMET	32, 11 (Specific, Parent)	Antarctica	Olivine-phyric shergottite	Enriched [#]	0.1253	18 [#]							5.8	0.2	3%	8.84	0.18	1527	54
LAR 12095	ANSMET	35, 27 (Specific, Parent)	Antarctica	Olivine-phyric shergottite	Depleted [#]	0.1781	16 [#]							5.8	0.1	2%	7.03	0.06	1204	28
RBT 04262	ANSMET	74, 57 (Specific, Parent)	Antarctica	Olivine-phyric shergottite	Enriched	0.1659	21.6	47.6	3.3	20.6	5.7	0.84	-6.7	4.1	0.1	3%	4.58	0.05	1104	35
Zagami	SM	MPI 632/8	Fall	Basaltic shergottite	Enriched	0.1535	11.3	50.5	6.1	18.1	10.5	0.83	-7.2	8.1	0.2	2%	8.53	0.08	1047	22
Y-000593	AMRC	131	Antarctica	Nakhlite(clinopyroxenite)		0.1835	10.4	47.6	1.9	19.7	14.3	4.24	16.9	9.3	0.1	1%	4.36	0.05	466	9
MIL 03346	ANSMET	74, 61 (Specific, Parent)	Antarctica	Nakhlite(clinopyroxenite)		0.1553	9.3	49.5	4.1	19.1	14.4	3.40	16.1	10.5	0.2	1%	10.63	0.09	1009	18
Nakhla	NHML	off BM.1913, 25	Fall	Nakhlite(clinopyroxenite)		0.1284	12.1	48.6	1.7	20.6	14.7	3.69	16.2	7.8	0.2	2%	6.03	0.12	775	23
ALH84001	ANSMET	321, 235 (Specific, Parent)	Antarctica	Orthopyroxenite		0.1217	25.0	52.8	1.3	17.5	1.8	0.46		7.2	0.2	3%	0.09	0.05	/	/
Mean values																			1082	
1s																			316	
number																			n=14	

*Cu and Ag contents were obtained from the same sample aliquots. Cu data have been reported before (Wang and Becker, 2017). Blank% means the percentage of subtracted total procedural blank.

Y-980459 and LAR 06319 possibly are the most primitive shergottites. Note their ratios are similar to the mean values.

#LAR 12011 is paired with LAR 06319 and LAR 12095 has a REE pattern similar to Sau 005 (Balta et al., 2015).

The La/Yb is CI chondrite normalized. The data source and major elements are from Herd et al (2013), Lodders (1998), Meyer (2013) and references therein. MgO with # symbol is assumed to similar in the pairs.

Initial ε¹⁴³Nd are from the literature (Debaille et al., 2009; Jones, 2015 and references therein).

ANSMET: Antarctic Search for Meteorites Program, NASA Johnson Space Center Houston and Smithsonian Institution, Washington D.C., USA

NHML: Natural History Museum, London, UK

AMRC: Antarctic Meteorite Research Center, NIPR, Tokyo, Japan

SM: Senckenberg Museum, Frankfurt am Main, Germany

Table 2. Comparison of Ag content data in the present study with literature values

Sample Name	Classification	This work			Literature					
		Ag (ng/g)	Cu ($\mu\text{g/g}$)	Cu/Ag	Ag (ng/g)	Cu ($\mu\text{g/g}$)	Cu/Ag	sources		
ALHA77005	Lherzolithic shergottite	4.8	4.35	903	4.4	5.4	1227	a		
					4.0			b		
					3.89; 4.85			5.41; 5.52	1115	c
Y-000097	Lherzolithic shergottite	1.9	2.65	1386	29	8.3	286	g		
Sau 005	Olivine-phyric shergottite	12.3	7.74	628	21	7.9	376	g		
Y-980459	Olivine-phyric shergottite	5.8	6.49	1122	68	6.2	91	g		
Tissint	Olivine-phyric shergottite	9.2	9.87	1077	46	12.5	272	g		
EETA 79001-A	Olivine-phyric shergottite	5.5	7.88	1428	19	10.4	118	a		
					5.3			b		
					88			g		
Zagami	Basaltic shergottite	8.1	8.53	1047	31	48.9	75	a		
					12.4			b		
					14.2			d		
					37			e		
					651			g		
Nakhla	Nakhlite	7.8	6.03	775	40	5.03	126	e		
					246			b		
					1380			d		
					32.1			f		
ALH84001	Orthopyroxenite	7.2	0.09	-	<0.9			b		
					0.22; 0.35			f		
Shergotty	Basaltic shergottite				37; 110	54	1459	a		
					203			11.9	59	e
					6.8; 10.5			26	2476	h
					16.9					d
					209			15.2	73	g

a: Smith et al. (1984); b: Kong et al. (1999); c: Biswas et al. (1980); d: Treiman et al. (1986); e: Laul et al. (1972); f: Wang et al. (1998); g: Yang et al. (2015); h: Laul et al. (1986)

Except data from Yang et al. (2015) by laser ablation ICP-MS, other Ag and Cu contents in literature were mainly determined by RNAA and INAA.

The Cu/Ag is calculated from literature data if both Ag and Cu data are available for the same sample aliquot.

Table 3. Silver and Cu contents in the analyzed ordinary chondrites.

Meteorites	WSG95300,68	Bremervorde	Ceniceros	Parnallee	Ochansk	Forest City	Mount Tazerzait	Saint Severin	Benguerir
Type	Find, H3.3	Fall, H/L3.9	Fall, L3.7	Fall, LL3.6	Fall, H4	Fall, H5	Fall, L5	Fall, LL6	Fall, LL6
Institution	ANSMET	USNM144	NHM London	NHM London	Com.	USNM 1649	Com.	USNM 6672	Com.
Mass (g)	0.0626	0.0570	0.0518	0.0463	0.0758	0.0555	0.0634	0.0553	0.0542
Cu ($\mu\text{g/g}$)	99.5	83.4	98.5	67.9	46.8	98.4	84.9	69.6	83.0
$\pm 2s$	1.0	0.8	1.0	0.6	1.1	1.0	0.9	0.7	0.8
Ag (ng/g)	23.4	227	39.9	40.9	42.1	63.6	75.3	34.9	30.6
$\pm 2s$	0.5	4	0.7	0.8	0.6	0.9	1.1	0.7	0.6
Cu/Ag	4257	368	2467	1660	1111	1548	1128	1992	2715
$\pm 2s$	106	8	51	35	30	27	20	42	62

Com.: commercial source